

## Possible Juventae Chasma subice volcanic eruptions and Maja Valles ice outburst floods on Mars: Implications of Mars Global Surveyor crater densities, geomorphology, and topography

Mary G. Chapman,<sup>1</sup> Magnús T. Gudmundsson,<sup>2</sup> Andrew J. Russell,<sup>3</sup> and Trent M. Hare<sup>1</sup>

Received 16 November 2002; revised 30 May 2003; accepted 10 July 2003; published 4 October 2003.

[1] This article discusses image, topographic, and spectral data from the Mars Global Surveyor (MGS) mission that provide new information concerning the surface age, geomorphology, and topography of the Juventae Chasma/Maja Valles system. Our study utilizes data from two instruments on board MGS: images from the Mars Orbiter Camera (MOC) and topography from the Mars Orbiter Laser Altimeter (MOLA). Within Maja Valles we can now observe depositional bars with megaripples that unequivocally show catastrophic floods occurred in the channel. Viking impact crater densities indicated the chasma and channel floor areas were all one age (late Hesperian to Amazonian); however, MOC data indicate a marked difference in densities of small craters between Juventae Chasma, Maja Valles, and the channel debouchment area in Chryse Planitia basin. Although other processes may contribute to crater variability, young resurfacing events in the chasma and episodes of recent erosion at Maja Valles channel head may possibly account for the disparate crater densities along the chasma/channel system. Relatively young volcanic eruptions may have contributed to resurfacing; as in Juventae Chasma, a small possible volcanic cone of young dark material is observed. MOC data also indicate previously unknown interior layered deposit mounds in the chasma that indicate at least two periods of mound formation. Finally, MOLA topography shows that the entire floor of the chasma lies at the same elevation as the channel debouchment area in Chryse basin, resulting in a 3-km-high barrier to water flow out of the chasma. Blocked ponded water would rapidly freeze in the current (and likely past) climate of Mars. For catastrophic flow to occur in Maja Valles, some process is required to melt ice and induce floods out of the chasma. We suggest subice volcanic eruption and calculate estimates of water discharges and volumes that these eruptions might have produced. *INDEX TERMS:* 6225 Planetology: Solar System Objects: Mars; 5470 Planetology: Solid Surface Planets: Surface materials and properties; 5480 Planetology: Solid Surface Planets: Volcanism (8450); 5416 Planetology: Solid Surface Planets: Glaciation; 5420 Planetology: Solid Surface Planets: Impact phenomena (includes cratering); *KEYWORDS:* jökulhlaup, tuya, tindar, chasma, volcanism, thermokarst

**Citation:** Chapman, M. G., T. M. Hare, A. J. Russell, and M. T. Gudmundsson, Possible Juventae Chasma subice volcanic eruptions and Maja Valles ice outburst floods on Mars: Implications of Mars Global Surveyor crater densities, geomorphology, and topography, *J. Geophys. Res.*, 108(E10), 5113, doi:10.1029/2002JE002009, 2003.

### 1. Introduction

[2] Juventae Chasma is a 180-km-wide (south end), 250-km-long depression northeast of the main interconnected troughs or chasmata of Valles Marineris, Mars (Figure 1). The Valles Marineris troughs have been generally interpreted as large grabens and (or) collapse structures, produced in association with tensional stresses generated by the Tharsis rise during the late Noachian to early Hesperian [Scott and Tanaka, 1986; Witbeck *et al.*, 1991;

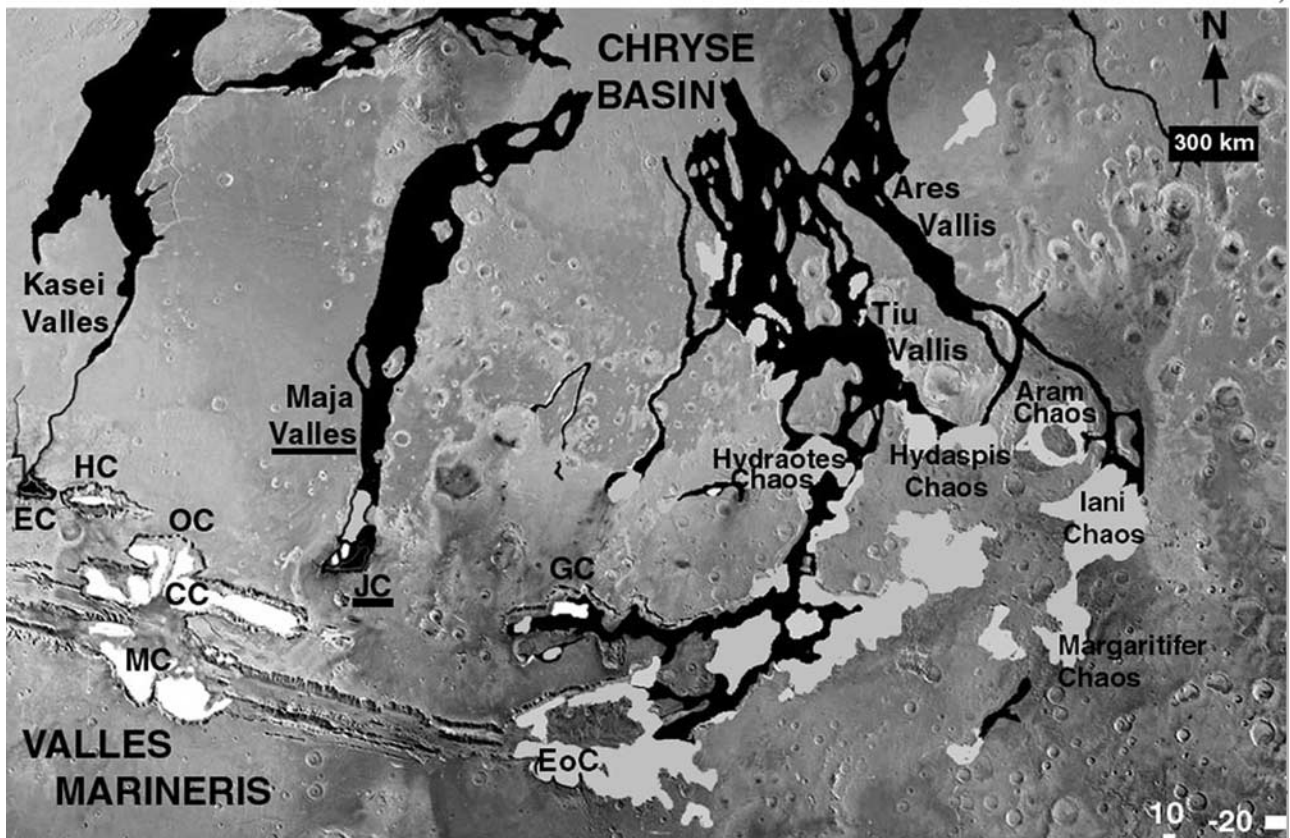
Tanaka *et al.*, 1991; Lucchitta *et al.*, 1992]. Dynamic upwarping and rising magma caused by a local mantle plume may account for the chasmata structures at Valles Marineris [Hartmann, 1973; Carr, 1974; Wise *et al.*, 1979; Anderson *et al.*, 2001; Chapman and Tanaka, 2002]. Chasmata floors contain interior layered deposit (ILD) mounds, dark materials, local areas of chaos, landslide deposits, and eolian materials. The chasmata and large confined areas of chaos, to the east, source the immense outflow channels that flow thousands of kilometers to the north to debouch into the northern plains of Mars. The origins of the ILDs and outflow channels are contentious, as are their relative ages and possible relations to each other, chasmata, and chaos. Juventae Chasma is the only isolated chasma that contains interior layered deposit (ILD) mounds, dark material, chaos, and connects to an outflow channel, Maja Valles. Maja is a

<sup>1</sup>U.S. Geological Survey, Flagstaff, Arizona, USA.

<sup>2</sup>Science Institute, University of Iceland, Reykjavik, Iceland.

<sup>3</sup>Keele University, Keele, UK.

a)



b)

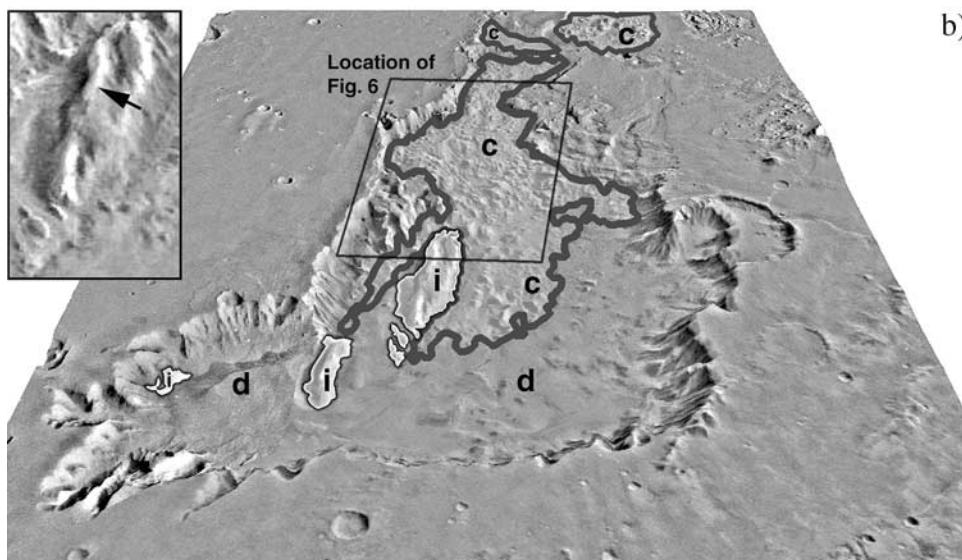


**Figure 1.** (a) Location map showing Valles Marineris troughs (EC, Echus Chasma; HC, Hebes Chasma; OC, Ophir Chasma; CC, Candor Chasma; MC, Melas Chasma; JC, Juventae Chasma; GC, Ganges Chasma; and EoC, Eos Chasma), and Chryse basin; outflow channels shown in black, interior deposits shown in white, and chaos shown in gray; Maja Valles and Juventae Chasma (JC) designations are underlined. (b) Oblique view of Juventae Chasma (south end width = 180 km) showing (in white) interior layered deposits mounds detected by Viking Observer Cameras (marked “i”), areas of chaotic blocks (marked “c”), and dark material (marked “d”); upper left corner inset shows largest mound with arrow that points to resistant caprock; image generated by draping Viking MDIM 2 over Mars Global Surveyor MOLA DEM.

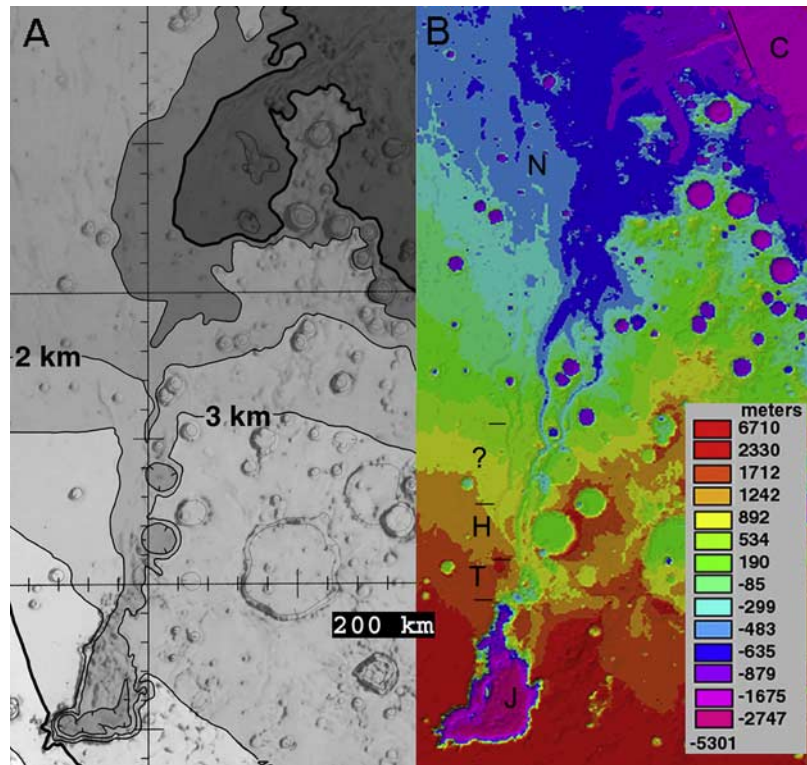


**Figure 2.** Topography of the Juventae Chasma and Maja Valles area derived from (a) Viking data having a 1 km contour interval and from (b) the Mars Orbiter Laser Altimeter. In Figure 2b: J, Juventae Chasma; T, transition zone from chasma chaos to nick point of Maja Valles; H, head of Maja Valles channel; question mark, area lacking MOC images on channel floor; N, north Maja Valles; and C, Chryse Planitia where Maja Valles terminates.

50- to 150-km-wide channel that extends northward from the box canyon of Juventae Chasma about 1600 km into the Chryse Planitia basin, where all traces of the flow are lost (Figure 1a). In order to understand the relations between source features and channel, we undertook an integrated MGS examination of this specific chasma-channel system. This article discusses the details of our findings and their implications.

[3] We begin the introduction with a brief review of knowledge gained from Mariner, Viking, and recent MGS data and the new interpretations from this investigation. From the early data sets we realized that the floor of Juventae Chasma contains chaotic blocks, ILD mounds, and dark materials (Figure 1b). Chaos consists of jumbled blocks of material that may be collapsed overburden materials due to the melting and destabilization of ground ice and expulsion of groundwater and rock debris [Sharp, 1973]. Chaos occurs mostly in the north half of the chasma. The ILDs are mesas or mounds consisting of layered materials having variable relative brightness. Detailed discussion of ILD characteristics suggested that the strongest hypotheses of ILD origin were either lacustrine or volcanic processes [Lucchitta et al., 1992; Komatsu et al., 1993]. Other workers have suggested a compromise origin, noting that certain aspects of ILDs are similar to terrestrial subice volcanic forms, such as tuyas and tindars, or volcanic edifices that form in meltwater lakes [Nedell et al., 1987; Croft, 1990; Lucchitta et al., 1994]. This Viking interpreta-

tion appears to be supported by MOC data [Chapman and Tanaka, 2001]. Viking-based studies showed that the large Viking-detected ILDs, within Juventae, overlie and are younger than chaotic blocks [Komatsu et al., 1993; Chapman, 2002]. This paper indicates previously unknown, small ILD mounds that predate chaos, indicating two periods of ILD formation in the chasma. Dark material within Valles Marineris was interpreted to be basaltic volcanic ash and stratigraphically very young, locally overlying ILDs [Geissler et al., 1990; Lucchitta, 1990]. However, vents could not be identified in Viking images. Possible small vents of dark material have recently been observed in MOC images [Chapman and Smellie, 2001; Lucchitta, 2001]. We observe a new MOC image that shows another small, young, possible volcanic cone of dark material associated with dark drifts and embaying an ILD mound within Juventae Chasma.

[4] Maja Valles (and the rest of the circum-Chryse channels) and the chasma floor areas were all mapped as one surface age and placed in the late Hesperian to Amazonian based on Viking impact crater densities [Scott and Tanaka, 1986; Witbeck et al., 1991; Rotto and Tanaka, 1995]. (The Martian system is divided into three epochs: Noachian (old), Hesperian, and Amazonian (young).) However, MOC data presented in this paper indicate a marked difference between densities of small impact craters on the materials of Juventae Chasma, Maja Valles, and the channel's debouchment area in the Chryse Planitia basin.

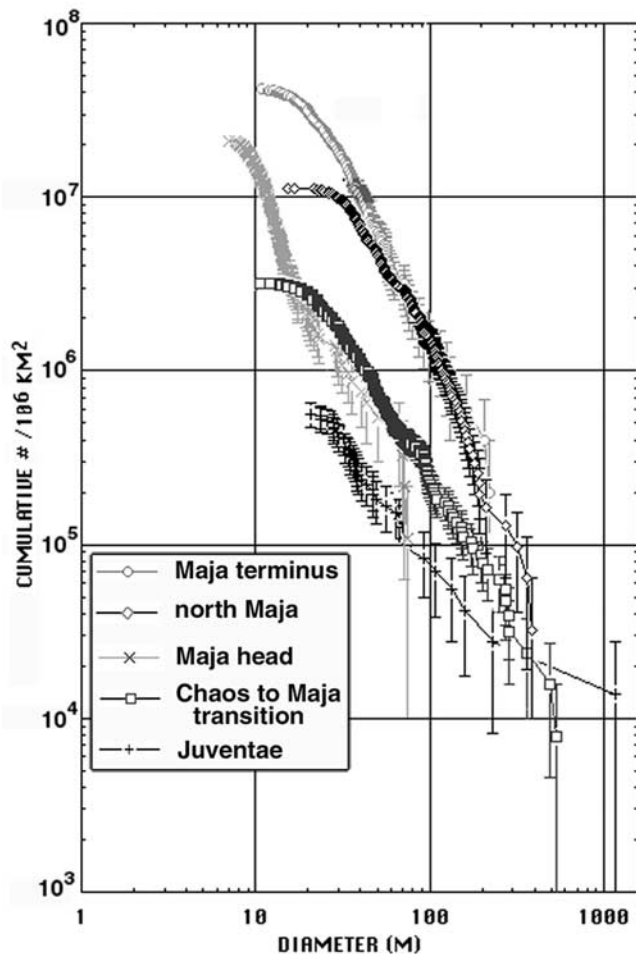


**Figure 3.** MOC meter-scale impact crater density curves for selected areas in Juventae Chasma and Maja Valles. For the Maja terminus area in Chryse Planitia, 177 craters were counted within a 4.92 km<sup>2</sup> area of MOC image M1000600; 221 craters were counted within a 30.72 km<sup>2</sup> area of M807135 in north Maja Valles; 147 craters were counted within a 9.2 km<sup>2</sup> area of M0300781 at the head of Maja Valles; 214 craters were counted within a 127 km<sup>2</sup> area of M0705846 in the transition area between chaos and the head of Maja Valles; and 36 craters were counted within a 71.71 km<sup>2</sup> area of M804669 in Juventae Chasma.

[5] Relations between ejecta from a 30-km-diameter impact crater and flood channel in Viking images near the channel terminus were cited as evidence that at least two episodes of Maja Valles channeling may have occurred [Greeley *et al.*, 1977; Baker and Kochel, 1979]. Downstream ponds in low catchment areas of Maja Valles and subsequent pond breaches were suggested to be the cause of these episodic floods in Chryse [Baker and Kochel, 1979; De Hon, 1992; Rice and De Hon, 1996]. MOLA topography, however, shows no downstream ponds within the low catchment areas of Maja.

[6] After the Mariner and Viking Missions, many origins for the outflow channels were suggested. Many researchers interpret the circum-Chryse channels to have had a catastrophic flood origin, based on their large streamlined mounds, conspicuous flow lines, and possible cataract

features [Milton, 1973; Baker, 1979; Baker and Milton, 1974; Baker and Kochel, 1979; Sharp and Malin, 1975; Masursky *et al.*, 1977; Carr, 1981]. Alternatively, Lucchitta [1982] proposed glacial erosion as a channel-forming process based on local U-shaped valleys in the upper reaches of some channels. Others have suggested that the channel features are the result of mass flows [Nummedal and Prior, 1981; Gooding, 1987; MacKinnon and Tanaka, 1989; Jöns, 1990; Tanaka, 1997]. Some authors proposed fretting by ground ice or groundwater sapping (modified by wind erosion) as alternative erosional processes [Sharp and Malin, 1975; Cutts and Blasius, 1981]. Recently, it has been suggested that magmatic intrusions may have mobilized subsurface CO<sub>2</sub> ice leading to eruption of the gas, chaotic collapse, and cryoclastic mass flows with extreme runouts [Hoffman, 2000; Tanaka *et al.*, 2002]. Although all of these hypotheses have their merits, this paper shows new MOC images that unequivocally demonstrate catastrophic floods occurred in Maja Valles and therefore that Juventae Chasma held a source of water or ice. On Earth, catastrophic floods on huge scale are formed only by outbursts of surface water dammed behind or underneath ice. Some of these floods, called jökulhlaups, are caused by rapid drainage of subice lakes, formed of meltwater derived from ice by volcanic eruptions. McCauley *et al.* [1972] and Masursky *et al.* [1977] suggested that the outflow channels were formed by jökulhlaups. Rice and Edgett [1997] made a case for comparing distal flood sediments in Chryse basin to similar sandur surface morphologies on Icelandic outwash plains formed by jökulhlaups. Unaware at the time of volcanic interpretations for ILD mounds or dark materials, Carr [1979] dismissed the jökulhlaup interpretation mainly on the lack of any evidence for contemporaneous volcanic activity in the chasmata and alternatively suggested that breaching of a confined subsurface aquifer may have produced water and generated the floods. However, we show that ILDs are aligned with structural features; this relation and existence of a possible volcanic cone of dark material (above) support the interpretation that volcanism occurred in Juventae. Chasma volcanism and new topographic data (below), resurrects the suggestion of jökulhlaups within Maja Valles.

[7] Viking topography indicated that most of the floor of Juventae lay upslope from the Maja channel [U.S. Geological Survey, 1989, Figure 2a]. New MOLA topography shows that the entire floor of the chasma lies at the same elevation as the debouchment area in Chryse Planitia (Figure 2b), resulting in a barrier to water flow out of the chasma [Chapman, 2001]. This creates a problem, although MOC images confirm that there were floods out of the chasma, the topographic low formed by Juventae Chasma would have likely prevented flow out of the chasma, and instead would have ponded water. In the current climate of Mars, the temperature ranged daily from about 200 to 260 K at the latitude-equivalent Pathfinder Lander site during the boreal summer and early autumn [Schofield *et al.*, 1997]. Assuming a similar climate in the late Hesperian to Amazonian, any ponded water would freeze within Juventae Chasma. We suggest heating from volcanic eruptions as a mechanism to drive water out of the chasma. Our calculated volcanically derived discharges and volumes are much

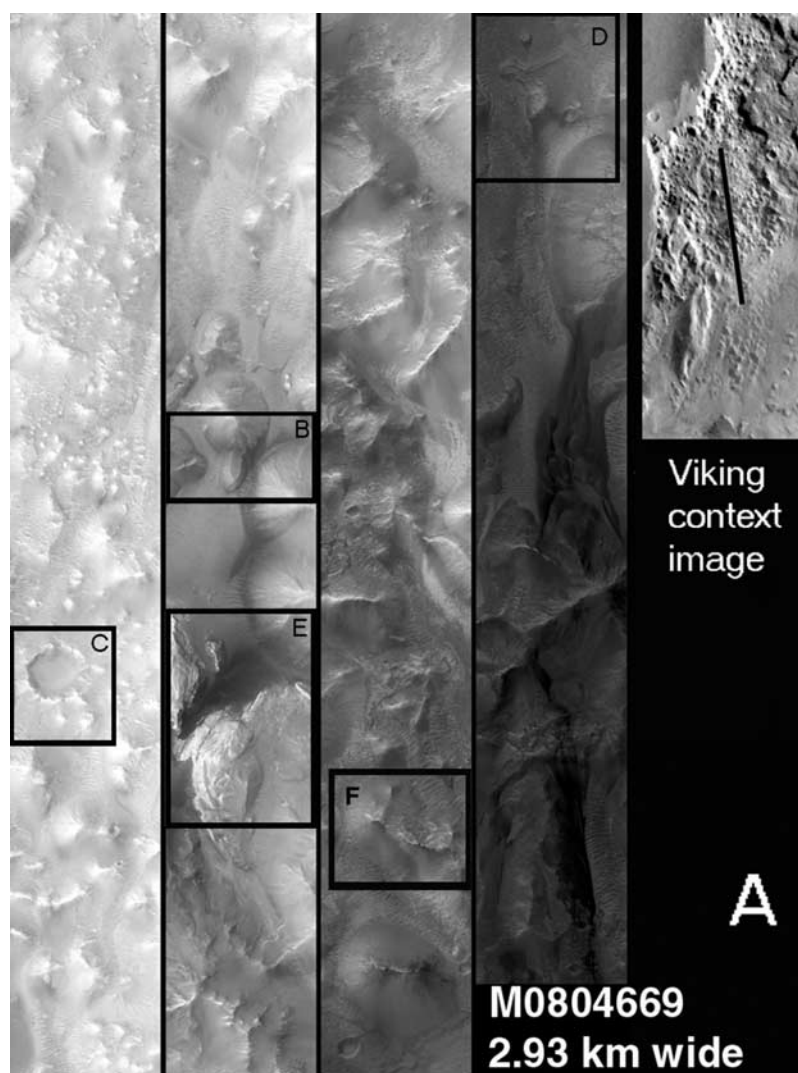


**Figure 4.** MOC image of M804669 within Juventae Chasma showing (a) entire sparsely cratered image tiles top (upper left; north) to bottom (right, south) with boxes denoting locations of B-F, and inset Viking context in upper right corner; (b) arrow marks dissected talus deposits on chaotic block (block lacks internal structures or bedding); (c) arrows mark possible thermokarst pits on ejecta blanket and rim of impact crater; (d) channel confined, dune covered material with box marking enlargement (below), that has arrows marking depressions (cracks) within material; (e) bright mounds are newly discovered small interior layered deposit mounds in Juventae Chasma (marked “i”) with arrow and contact line marking overlying chaotic block material (marked “c”); (f) similar to wallrock, the chaotic block has apparent layers (marked “L”) and a rocky spur (arrows).

lower in volume than those that are generated from topographic studies of the channel.

## 2. MOC Cratering Densities and Geologic/Geomorphologic Relations

[8] In our preliminary study of the Juventae Chasma and Maja Valles system, an observational scan of all released MOC narrow angle (N/A) images (between September 2001 and the submission date of this article) showed an apparent marked difference in densities of small (<500 m) craters along the chasma/channel system. These small craters can be used to create measurements of the most geological recent “activity rate” that characterize planetary surfaces

[Hartmann, 2002]. To statistically confirm our visual observation of surface differences, crater counts were made within five individual MOC N/A images in each of the five regions of apparently different cratering densities along the system (Figure 3). We wanted to date the age of channel resurfacing, so in Maja Valles, craters were counted only on channel floor areas, not on surfaces of kipukas or inselbergs above erosion level. However, all craters in Juventae Chasma were counted. As there are no large, young, nearby craters within several crater diameters of the chasma-channel system, none of the craters we measured appeared to be secondary impacts. The cumulative densities for craters with diameters  $>50 \text{ m}/10^6 \text{ km}^2$  show that the chasma floor/chaotic areas ( $167 \pm 48$ ) have a paucity of pristine

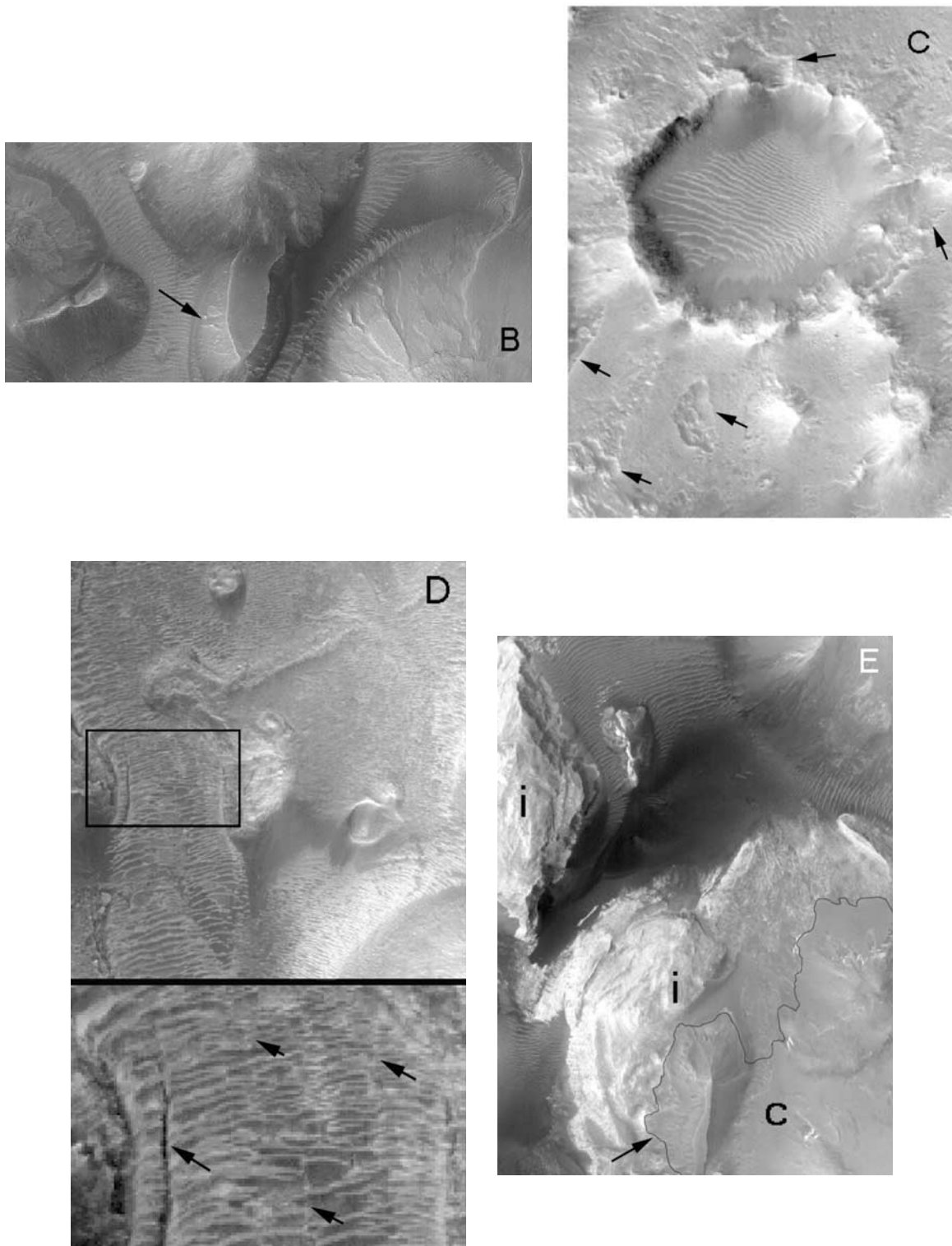


Figure 4. (continued)

impact craters with respect to other areas. The transition area from chaos to channel ( $700 \pm 74$ ) and channels directly north of the chasma ( $543 \pm 243$ ) are also sparsely cratered. However, from about 300 km north of the chasma, the Maja channel area is more heavily cratered ( $4524 \pm 383$ ), as is the Chryse basin floor ( $6224 \pm 1118$ ). We examined all of the

images in each of the five areas in order to explain the incongruent surface ages.

### 2.1. Juventae Chasma

[9] No large landslides or obvious mass-wasting deposits, which could bury floor areas, have been mapped within

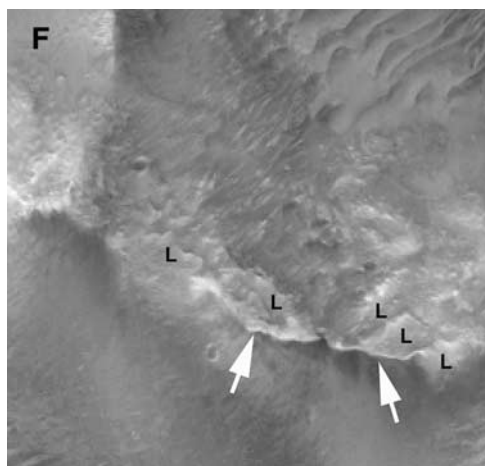


**Figure 4.** (continued)

Juventae Chasma. At the MOC scale, surfaces within the chasma have few impact craters, indicating a very young surface age (Figure 4a). In addition, MOC image M0804669 shows some interesting geologic/geomorphic relations that occur within the chasma (Figure 4a). For instance, on the south side of a chaotic knob, a talus deposit with a flat, possible pediment cap has been cut by late-stage erosion from wind, water, or ice (Figure 4b). This relation indicates that relatively steady, talus-forming erosion was interrupted by a period of downcutting that incised the talus and caprock. On the north part of image M08-04669, an impact crater rim and its ejecta blanket are pitted with irregularly shaped depressions that appear similar to terrestrial thermokarst pits found in active glaciated and periglacial terrain due to the meltout of buried ice [Sugden and John, 1976; French, 1996] (Figure 4c). The south end of this same image shows possible brittle fracture of channel-confined, dune-covered material (Figure 4d). The possible thermokarst pits and brittle fractures may indicate melting of late-stage ground ice. We knew from Viking imagery that there were three ILD mounds in Juventae Chasma (marked “i” on Figure 1b). The largest mound (Figures 5 and 1b) embays nearby chaotic blocks, indicating it formed after chaos development [Komatsu *et al.*, 1993; Chapman, 2002]. However, MOC image M0804669 shows that north of this large mound, previously undetected, small ILD mounds (marked “i” on Figure 4e) appear to be superposed by chaotic blocks and hence may predate the chaos. Therefore at least two periods of ILD or chaos formation occurred in Juventae Chasma. MOC images show at least two types of chaotic blocks or knobs in the chasma: (1) friable material knobs with no discernible internal geomorphic attributes (Figures 4b and 4e), and (2) knobs that look like blocks of wallrock having layers and rocky spurs (Figure 4f).

[10] The large ILD mound trends N-S (Figures 1b and 6), matching the trend of the chasma as well as that of a depression internal to the mound (Figures 5 and 6). A 3-D chasma view of MOLA topography combined with MOC wide-angle image mosaics shows a linear depression (graben?), with the same N-S trend, trailing north away from the large ILD mound along the length of the chasma (Figure 6). The newly discovered small ILD mounds lie just east of this depression along a NW-trending lineation (fault)

that cuts the N-S depression. Alignment of the mounds with these surrounding possible structural features suggests tectonic control for mound placement, supporting an interpretation that the ILDs may be volcanic.

[11] MOC image M1000466 shows a cone of dark material with a central depression that embays the smallest Viking-detected ILD mound on the southwest wall of Juventae Chasma (Figure 7). The cone has a central, elevated depression (caldera?) and what appear to be smaller vents aligned in a linear trend off the flank of the cone. With no apparent superposed impact craters, the cone appears to be very young. If the cone is a volcano, this would provide a potential source for some of the dark, essentially impact-crater-free (hence young) material (marked “d” in Figure 1b) that forms large dunes and mantles on local areas of the chasma floor.

[12] Collectively, the image data imply that the very young age of the Juventae Chasma floor can be explained by a combination of late-stage flood erosion, thermokarst disruption by melting of later-stage ground ice, and/or young volcanic activity. In addition, friable (i.e., easily eroded by the wind) target rocks could also produce a paucity of impact craters in the chasma, as well as some



**Figure 5.** Viking Orbiter image showing largest interior layered deposit mound in Juventae Chasma (also shown on Figure 1b inset); arrow marks mound fork around underlying chaotic block; north toward top.

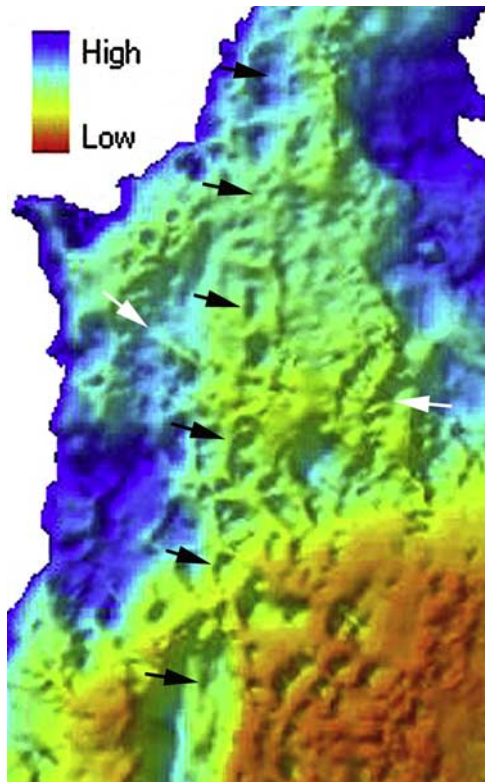


**Figure 6.** Three-dimensional view of MOLA data showing lineations within Juventae Chasma; black arrows denote N-S trending lineation extending north from trough in largest ILD mound; white arrows mark either end of E-W trending lineation; north toward top; location of image shown on Figure 1b.

material (subsequently removed) that protected the area from impacts, and burial by recent eolian deposits.

## 2.2. Maja Valles Channel Head

[13] The transition zone of the channel is here defined as the area from the last chaotic blocks to the incipient nick point of the Maja channel (marked “T” on Figure 2b). This transition zone and the first 100 km of the channel (past the nick point, marked “H” on Figure 2b) have overlapping crater count curves and so essentially the same surface ages (Figure 3). MOC images in the transition area show that most impact craters are either breached by erosion or occur on high ground, i.e., on noneroded inselbergs (Figure 8). The low channel floors contain very few impact craters at the MOC scale. A bit farther down the channel, image M0300781 shows a streamlined island, topographically higher than the low channel floor, with a 2-km-diameter breached impact crater on its stoss side (Figures 9a and 9c). A similar breached volcanic crater with a leeward depositional bar can be observed in the Jökulsá á Fjöllum flood channel in northeast Iceland (Figure 10). However, without the resolution to observe bedforms and on the basis of gross surface morphology alone, it is impossible to tell erosional islands from depositional obstacle-related bars [Allen, 1984; Russell, 1993]. Therefore the lower lee side of the island may be an erosional remnant or a depositional bar. Small MOC-sized (20–100 m diameter) craters occur mostly

north on the lee side of the island (Figure 9b) and on the 2-km-diameter crater rim (Figure 9c). Only a very few small (<10 m) craters occur on the channel floor. Small impact craters superposed on the 2-km breached rim are not breached, but show some degradation consistent with wind erosion (buried or absent ejecta and fill of crater floors). However, all the small craters on the island are breached and have more eroded rims. The cratering history and breached craters suggest at least two erosional episodes. Early erosion had a high enough level to breach the 2-km-diameter crater. Later erosion had levels that overtopped the lee side of the island to cut craters there, but did not reach the topographic height of the unbreached craters on the 2-km-diameter crater rim. Logic demands that the two erosion episodes be separated by enough time to form the small craters on the island.

[14] Our evaluations of the channel head area suggest that its young crater retention age may be due to episodes of relatively young channel erosion. The lack of craters on the nearby channel floor and farther south at the channel head suggest the last episode was relatively recent. In addition to channel-forming erosion, surface modification at the channel head may have been complemented by having friable target rocks on the channel floor, eolian erosion of the friable rocks, and eolian mantling of topographically lower channel areas. However, a strong role for eolian mantling is doubtful, as channel features are observable through the thin dune cover on the channel floor.

## 2.3. Topographic Estimate of Maja Valles Discharge Values

[15] The M0300781 streamlined island (discussed above) is just north of Juventae Chasma within the headward area of Maja Valles, through which passed all of the water from the Juventae source. We can estimate maximum discharge from Juventae Chasma from the island’s geologic history of two erosion episodes, MOLA profiles across this headwater area, and use of the Chezy equation [Chow, 1959] adapted for Mars gravitational acceleration of  $3.8 \text{ m/s}^2$ :

$$Q = (0.51/n)AR^{2/3}\theta^{1/2}, \quad (1)$$

where  $Q$  is the discharge in meters/second,  $A$  is the cross-sectional area of the channel,  $n$  is the roughness coefficient,  $R$  is the hydraulic radius, and  $\theta$  is the slope. Carr [1979] and De Hon and Pani [1993] performed similar derivations on downstream areas of Maja Valles using Viking topography and image feature morphometries, and estimated discharges between  $7 \times 10^6$  to  $5 \times 10^8 \text{ m}^3/\text{s}$  and  $62 \times 10^6 \text{ m}^3/\text{s}$  to  $84 \times 10^6 \text{ m}^3/\text{s}$ , respectively. For the later flood episode that overtopped the lee side of the island, the MOLA determined height is 440 m above the lowest channel depth and the horizontal width of the channel is 34 km (Figure 11). The height of the 2-km crater can be used as a minimum value for a maximum discharge, as breaching indicates the highest flood level was at least at the crater rim and possibly a bit higher (although not too much higher, as craters above this level are not breached). The 2-km crater, breached in an early flood, is 589 m above the base of a 41-km-wide channel (Figure 11). Using these water column heights, channel widths, and MOLA channel slopes adjacent to the island, GIS methods produce the wetted cross-sectional



**Figure 7.** MOC image of M1000466 showing small dark cone superposed on bright material of interior layered deposit mound, located on southwest wall of Juventae Chasma (Viking context image inset); black arrow marks central topographically high depression (caldera?); white arrows mark smaller depression aligned in chains on the flank of cone; note absence of impact craters; north toward top.

area and the hydraulic radius from which the program calculates possible maximum discharges of  $2 \times 10^8 \text{ m}^3/\text{s}$  and  $4 \times 10^8 \text{ m}^3/\text{s}$ . These discharges are within the upper limit calculated by Carr [1979]. Use of the Chezy equation is appropriate to estimate discharge on established channels at bank-full flow. However, the derived flow speeds must be considered maximum estimates because the true base level at the time of flooding is unknown. In addition, Maja Valles is a deeply channeled valley that may have experienced several periods of downcutting; MOC images suggest at least two events (see above). Rather than estimating discharge using the Chezy equation, we suggest that modeling channel flow on processes related to terrestrial catastrophic flow channels (section 3.1) may provide more accurate estimates of discharge values.

#### 2.4. Maja Valles Downstream

[16] To describe the rest of the channel, we follow the established format of terrestrial river description using

mileposts or kilometers down channel, which in the case of Maja Valles is to the north. Our beginning point, or km point 0, is the farthest northern extent of Juventae chasma.

[17] As of the submission date of this paper, there are only two MOC images of Maja between the km 100 point (100 km north of Juventae Chasma) and about the km 230 point (area marked “?” in Figure 2b), and these images are not located in the channel floor proper. MOC images from km 230 and northward on Lunae Planum (area marked “N” in Figure 2b) show a much more heavily cratered surface here than the channel head to the south. For example, compare equal areas of image M08-07135 on a streamlined island (topographically above the lowest levels of erosion) and on the channel floor (Figure 12a). Although, compared to the floor (Figure 12d), some craters on the island (Figure 12c) have larger diameters (300 to 500 m), both areas show numerous craters at the MOC scale. Closer inspection, however, indicates many odd craters on the channel floor area that are densely

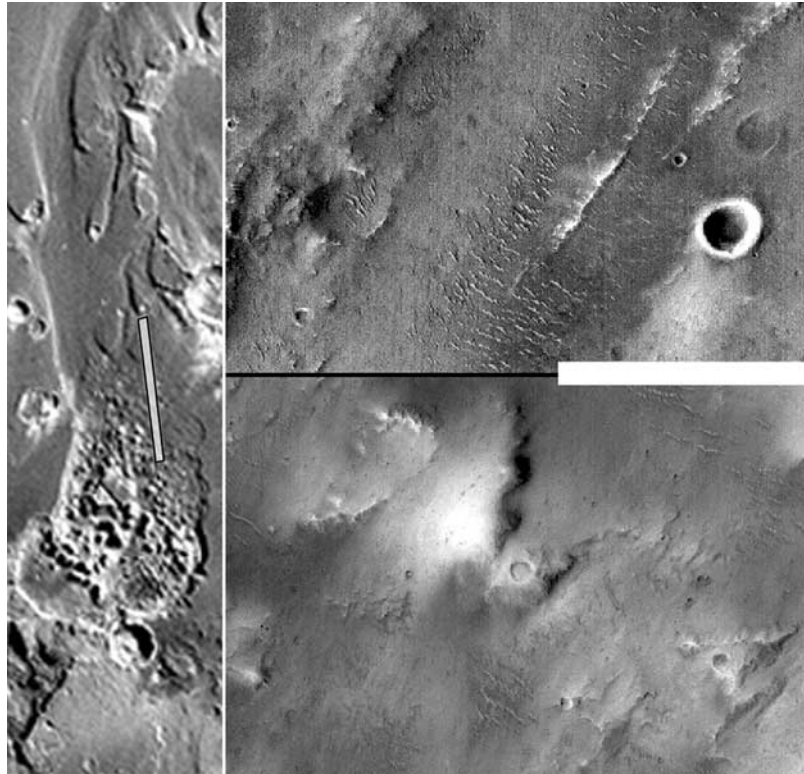


**Figure 8.** MOC image M0705846 in the transition area between Juventae Chasma and Maja Valles (left); equal area enlargements of image (right) show that most impact craters are either breached by erosion and partly buried or occur on high ground, i.e., on noneroded inselbergs; note that low channel floors contain very few impact craters; 1 km scale bar shown in white; north toward top.

packed and have irregular, noncircular rims (Figure 12d). It is possible that some of these depressions are not impact craters. For example, image M10-02524, shows irregularly shaped, rimless, white-floored craters, lacking discernable ejecta (Figure 13a). These craters are visually very similar to rimless kettle holes formed by melting of flood-deposited ice blocks [Fay, 2002a, 2002b, Figure 13b]. In addition, MOC SP2-36403 appears to show circular depressions surrounding small blocks, some infilled by bright material (Figure 14). If channel erosion was due to flooding, these may be obstacle marks. Catastrophic flood materials such as high-energy jökulhlaup deposits commonly display obstacle marks associated with scour around ice blocks and other boulders [Russell, 1993; Russell and Knudsen, 2002; Fay, 2002b]. Obstacle marks form a moat, caused by current scour around blocks and boulders. If the obstacle was an ice block, subsequent block melting, could form pits that may be mistaken for impact craters.

[18] The older surface age of heavily cratered channel floors in relation to young headwater areas could be accounted for if (1) few young flood events reached these channel extents, (2) young erosional events in these wide channel areas either lacked the power to remove craters or the sediment load to bury them, (3) craters were protected from erosion by ice infills, (4) downstream target rocks were less friable (hence not as easily eroded by wind), and/or (5) not all of the circular depressions that were counted as craters are due to impacts.

[19] Although origins other than catastrophic floods have been suggested for the outflow channels, a new finding

from the MOC images in the mid-channel part of Maja Valles provide clear-cut evidence for large-scale fluvial processes. A few images on the channel floor, including M15-00976, show longitudinal deposits with superposed megaripples (Figure 15a) that display an identical morphology to megaripple bedforms on giant depositional bars from Holocene Icelandic floods [Chapman and Russell, 2001, Figure 15b]. The presence of large-scale bars with megaripples, obstacle marks and kettle holes are unequivocal evidence of large-scale turbulent fluid flows. These rippled bars could therefore not be formed by glacial erosion, debris flows, fretting, sapping, or cryoclastic flows. The bars are fairly heavily cratered at the MOC scale and therefore are older features that did not result from the youngest floods out of Juventae Chasma. The bars occur beyond km 300, where the channel widens. Lateral flow expansion at km 300 may have reduced flood bedload transport capacity downstream.

## 2.5. Chryse Planitia Channel Terminus

[20] The floor of Chryse basin, just east of the mouth of Maja Valles (area marked “C” in Figure 2b), contains streamlined islands carved by flow from the channel. Although error bars overlap, crater counts in this area indicate a surface age that is older than the north (downstream) channel area on Lunae Planum (Figure 3). Unlike the north reaches of the channel, the Chryse craters are mostly pristine with few irregular depressions that may have resulted from other processes. For example, MOC image M10-00600 is not on a topographically higher inselberg, but

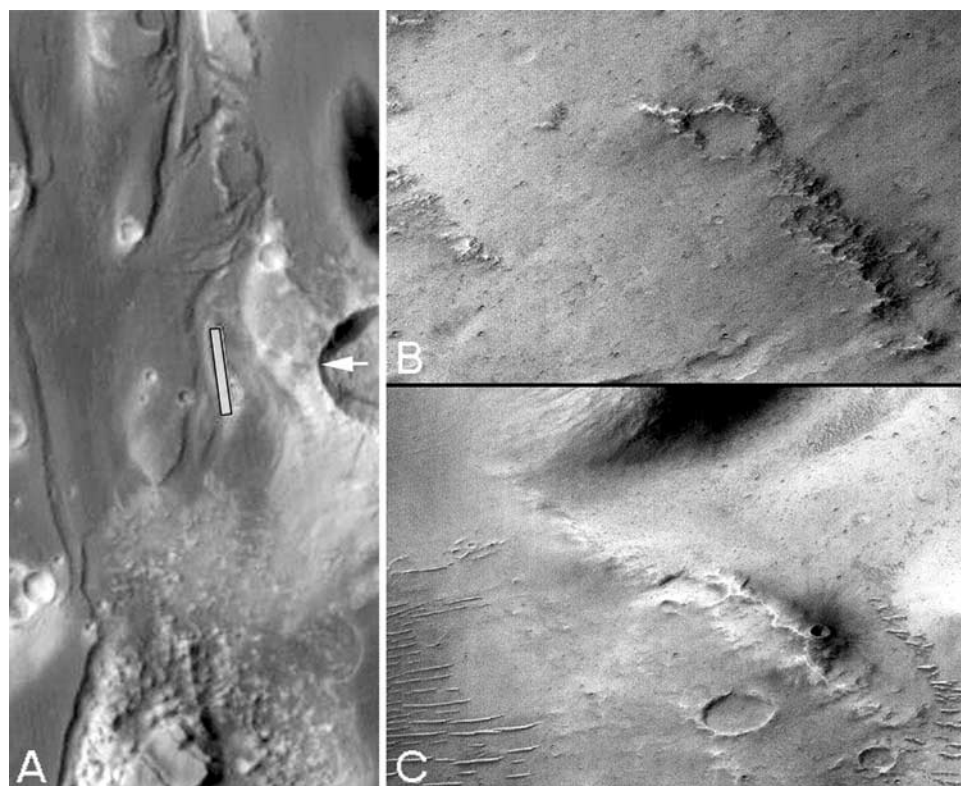


**Figure 9.** MOC image M0300781 lies over a streamlined island (also shown in Figure 11), topographically higher than the low channel floor, in the headwater area of Maja Valles (a) arrow marks crater shown in Figure 11; (b and c) equal area enlargements of image show the north, lee side of the island (Figure 9b) and breached rim of a 2-km-diameter impact crater on the stoss side of island (Figure 9c); note small (20–100 m diameter) craters mostly on the 2-km-diameter crater rim, and eroded small craters on the lee side of the island; image and enlargements are 1.48 km wide; north toward top.

located just west of the stoss side of a streamlined island in an area that was carved by floods (Figure 16). This image shows numerous impact craters <20 m in diameter, with pristine rims. Like the northern channel area, there is no evidence that young floods reached the extent of the heavily cratered, streamlined, Chryse area.

[21] The early interpretations of at least two episodes of Maja floods that affected Chryse Planitia were Viking-based [Greeley *et al.*, 1977; Baker and Kochel, 1979]. As the Viking craters indicate a late Hesperian age and as the Chryse basin area is heavily cratered at the MOC scale, the floods that likely reached the basin were all older, Upper Hesperian events. Breaching of ponds in large catchment basins of northern downstream Maja Valles was suggested as a means of generating the episodic floods in Chryse Planitia [Baker and Kochel, 1979; De Hon, 1992; De Hon and Pani, 1993]. Initial floods were suggested to drain through older Vedra and Maumee Valles [Greeley *et al.*, 1977; Theilig and Greeley, 1979]. Later breaching of these hypothetical ponds supposedly led to stream capture by Maja Valles [Baker and Kochel, 1979; De Hon, 1992; De Hon and Pani, 1993]. However, MOLA does not show evidence of fluid catchment areas on this section of north (downstream) Maja Valles, as there are no large areas within closed contours that would indicate topographic basins (Figure 17). Only one small, enclosed basin (marked “b” on Figure 17) occurs at the head of Bahram Vallis, a

theater-headed channel that may have formed by spring sapping of water from saturated upstream areas. Breaching of this small basin would only have drained a very limited amount of fluid into Bahram Vallis. Other larger area topographic contours are not closed. Rather than ponding, the open contours of the MOLA data, that gradually decrease in elevation toward the drainage channels, appear to support broad sheet wash from overland flow cutting Maumee and Vedra Valles during highstands and being confined to Maja during low stands. Old episodic channel scour by Maja Valles may have been due to multiple floods in the late Hesperian.

[22] Much of the sediment deposition from the old outflow episodes may have occurred upstream in Maja Valles on Lunae Planum, beyond km 300 in the area of the heavily cratered megaripple channel bars. Therefore the streamlined island area of Chryse Planitia adjacent to Maja may only contain a thin cover of fluvial sediments. The planitia islands may be erosional features and removed sediment may be located farther north in the lowlands of Mars.

### 3. Chasma/Channel System Topography: Floods From a Frozen Hole?

[23] Viking images of the outflow channels show no features interpreted as glacial moraines. Viking topography

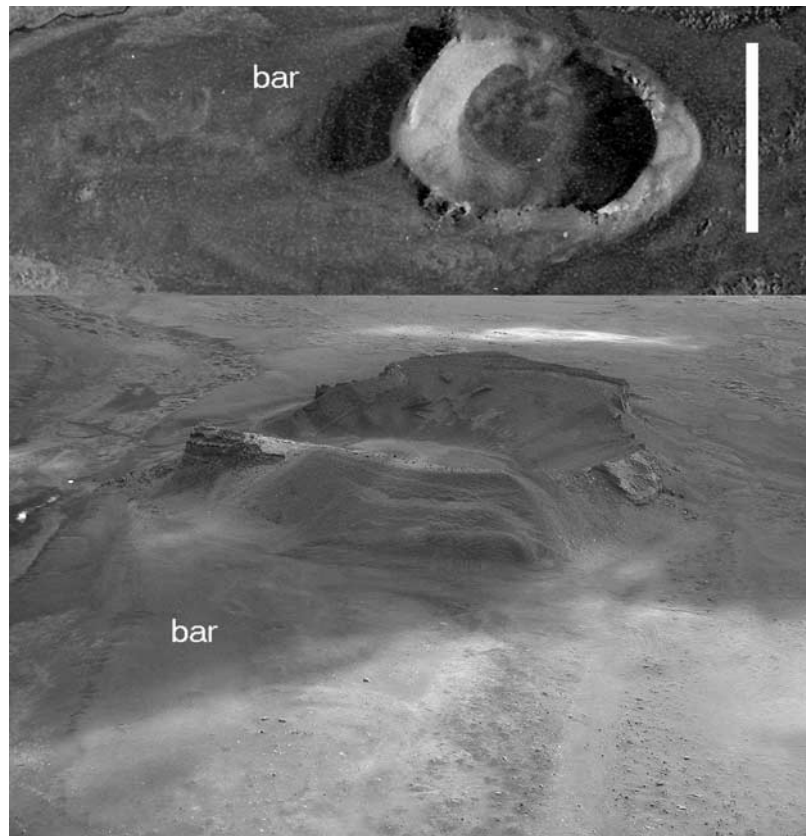


**Figure 10.** Areal photographs of Hrossaborg, a breached volcanic crater with a leeward depositional bar in the Jökulsá á Fjöllum, a flood channel in northeast Iceland; plan view (top; 250 m bar for scale), oblique view (bottom).

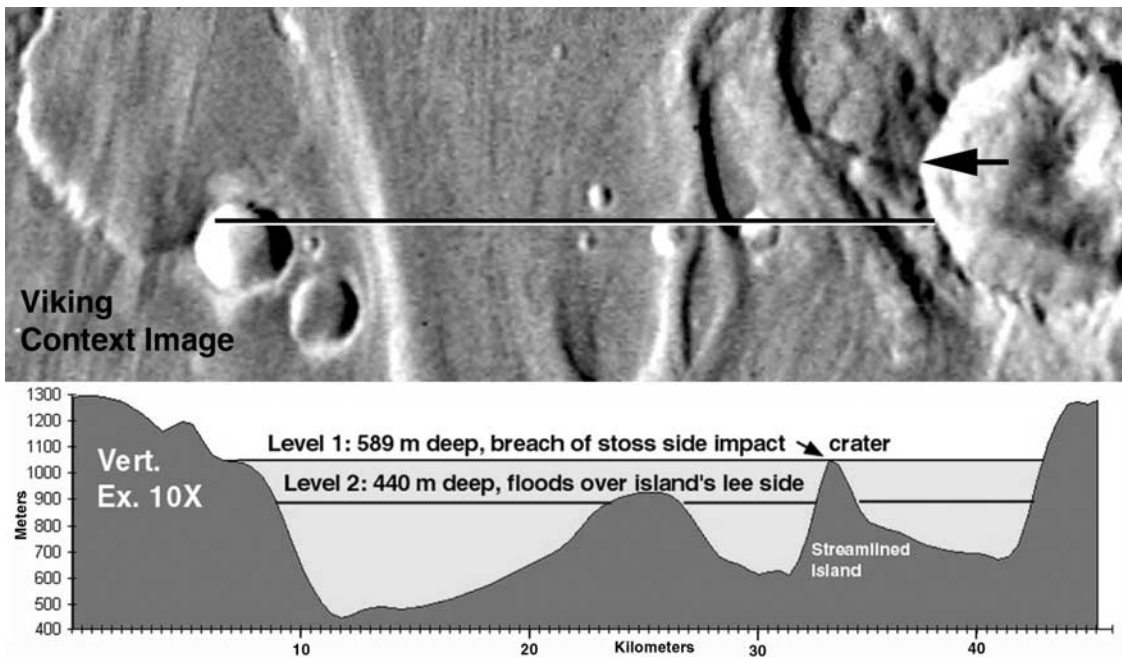


**Figure 11.** Image showing Viking Context image of Maja channel at latitude of streamlined island on Figure 9 with location of MOLA topographic profile (top; arrow marks crater shown in Figure 9; north toward top) and schematic image (bottom) showing computed profile of wetted channel perimeters of flood levels that overtopped island's 440-m-high lee side and the 589-m-high, 2-km-diameter crater rim stoss side.

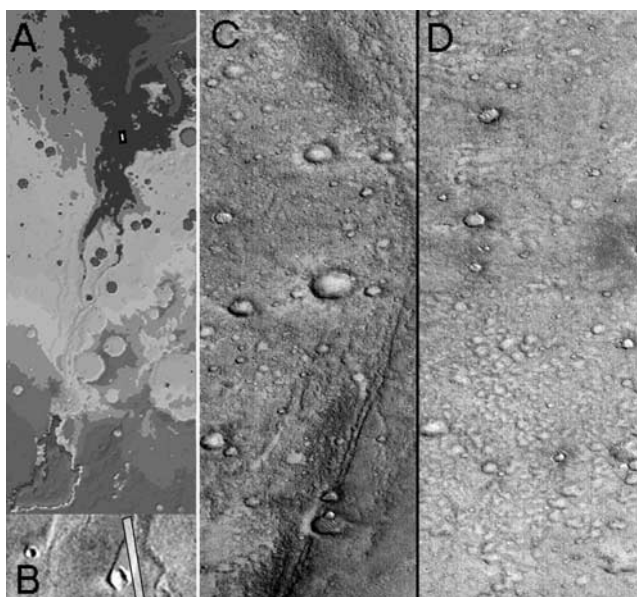


**Figure 12.** Image showing (a) location of MOC image M0807135 in north Maja Valles on MOLA context image; (b) image across streamlined island on Viking context image; note density of impact craters on equal 1.5-km-wide areas of (c) streamlined island and (d) adjacent floor; north toward top.

indicated Juventae Chasma lay topographically upslope from Maja Valles and had a volume of  $62,500 \text{ km}^3$ , and a floor about 2.5 km deep [U.S. Geological Survey, 1989, Figure 2a]. On the basis of this data, Carr [1979] hypothesized that Maja floods, rather than being related to surface ice, more likely resulted from a breach of a confined aquifer underground below Juventae Chasma. However, new high-resolution MGS data alter the previous assumptions about the chasma. MOLA data indicate the floor of Juventae Chasma lies topographically below Maja Valles, at elevations equivalent to the Chryse basin channel sink (Figure 2b). At  $113,275 \text{ km}^3$ , the volume of Juventae Chasma is much larger than previously thought. Relative to the plateau walls and at its lowest point, the chasma floor is about 6 km deep,  $-3.3$  km below datum. The Maja channel head lies at about 100 m above datum.

[24] MOLA data show an uphill gradient (3 km rise over 150 km run) in Juventae Chasma. Any water exiting the Chasma would be blocked by a 3-km barrier to water flow. Carr [1979] noted that rupture of an aquifer would cause water to be pumped only to the surface and would not result in overflow. Although water freed from a confined aquifer may have repetitively filled the chasma [Carr, 1979], it could not erupt with enough force to propel itself over 3 km up and out of the chasma. Any accumulating water would be confined to the enclosed depression to pond and freeze, assuming a Mars climate similar to the present in the late Hesperian to Amazonian. Confined to the chasma, this ice would be unable to move downslope and at summer temperatures ranging from 200 to 260 K [Schofield *et al.*, 1997], it would likely be cold-based. As previously discussed, MOC shows features such as flood bars, obstacle marks, and kettle holes that indicate Maja floods truly flowed from the chasma. To generate these floods, some process had to melt the confined ice and hydrostatically drive the water uphill out of the chasma. On Mars, this

process could be induced by the subsurface rise of magma. The chasma may have had any one of several origins. However, the association of catastrophic floods, ice ponded in a volcano-tectonic chasma setting, and possible volcanic material in the chasma leads us to suggest subice volcanism as a possible process to generate Maja jökulhlaups.

[25] Terrestrial subice volcanic eruptions melt ice and generate unstable meltwater lakes, which drain suddenly as jökulhlaups. The direction of flood flow is controlled by the gradient of an overlying ice sheet. Upslope flow can occur beneath temperate glaciers because the slope of the bedrock and the slope of the overlying ice surface determine the gravity potential [Paterson, 1994; Björnsson, 1988]. This type of event occurred in association with the 13-day-long fissure eruption in Gjalp, Vatnajökull, Iceland in October 1996 [Gudmundsson *et al.*, 1997; Chapman *et al.*, 2000]. Significant storage of meltwater did not occur at the eruption site of Gjalp, since the water flowed up and over a bedrock topographic obstacle into the Grímsvötn caldera lake for 5 weeks before it was released in a very swift jökulhlaup [Gudmundsson *et al.*, 1997].

[26] MOC shows the largest ILD mesa in Juventae Chasma to have a central high mesa with thin, eroded caprock (inset Figure 1b). The smaller mounds are uncapped. If the mounds are subice volcanoes, then the height of the large capped mesa can be used as a rough maximum value for the height of ponded ice within Juventae Chasma. This is because subice volcano, tuya and tindar components are formed in three sequential stages: (1) pillow volcano, (2) tuff cone, and (3) lava cap [Jones, 1969, 1970; Gudmundsson *et al.*, 1997]. Effused subaerial lava caps a mound when the volcano rises above the level of the meltwater lake that is close to, but below the level of the ice. Therefore the thickness of an ice sheet can be roughly estimated from the height of a tuya/tindar lava cap, as it can be as high or higher than the thickness of the

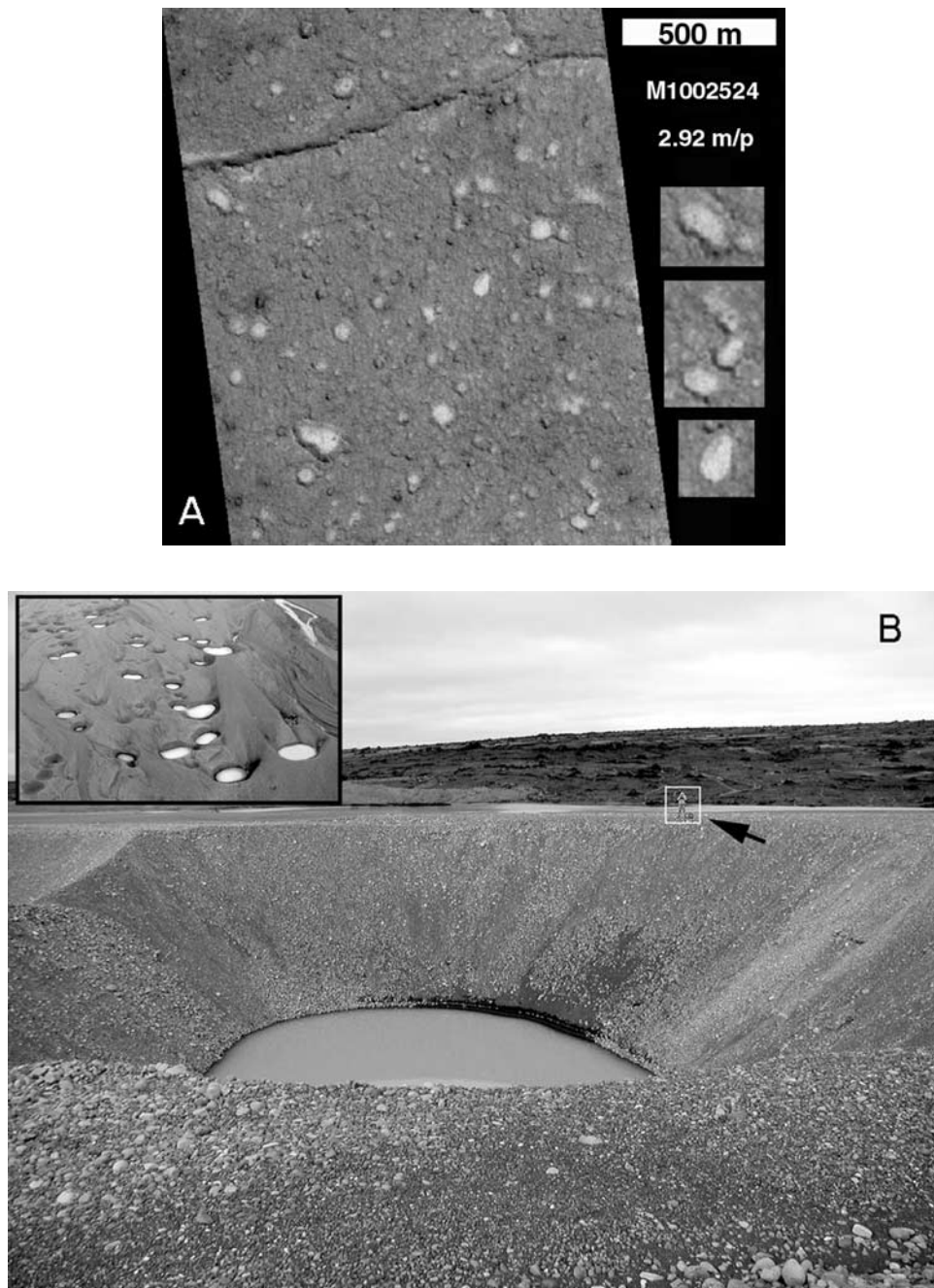


**Figure 13.** (a) MOC image M10-02524 showing irregularly spaced, white-floored depressions that appear to have trends parallel to that of flood-carved ridge at top of image; enlargements of selected depressions on right; north toward top. (b) Photo of 100-m-diameter kettle hole at Skaftafell, Iceland; arrow points to boxed human scale; inset (upper left) shows air photo of kettle hole field. Greenish-white water from melted ice block in the kettle ponds are colored by their content of glacial rock flour and clay.

surrounding ice and used as a rough maximum value for ice thickness [Chapman, 1994].

[27] The large Juventae ILD mound resembles a capped tindar (hyaloclastic ridge). MOLA topography indicates that this mound is about 2 km high, with the highest point reaching an absolute elevation of about +80 m (on an E-W profile, the elevation of the surrounding plateau walls is about +1900 m; Figure 18). Using GIS to infill the depression of Juventae Chasma and the head of its outflow channel Maja Valles to a lid of this altitude indicates that all source

locales, areas of chaos in Juventae Chasma and basins downstream, lie below +80 m of elevation (Figure 19a). Maja Valles and its streamlined features lie above this elevation, appearing just at the +80 m contact, a finding that supports the interpretation of direct relations between the mound, ice volume, and the floods. The maximum volume of ice, within Juventae, below the elevation of +80 m is 56,423 km<sup>3</sup>. The bottom of the ice fills a surface with a gradient that slopes uphill to the north, out of the chasma (Figure 19b).

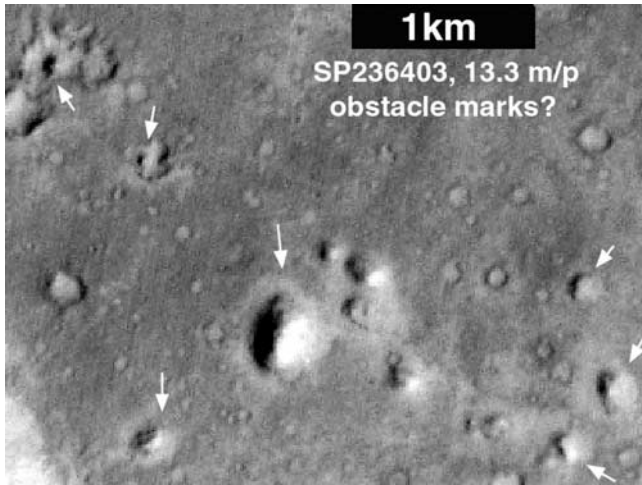


**Figure 14.** MOC image SP2-36403 showing small block surrounded by circular depression of the floor of Maja Valles; north toward top.

[28] On the basis of our estimates of GIS measurements of MOLA data, we suggest conservative volumes of the three Viking-detected ILD mounds (from northeast to southwest) are  $1542 \text{ km}^3$ ,  $381 \text{ km}^3$ , and  $84 \text{ km}^3$ . The newly discovered mounds are too small for accurate MOLA derived volumes. Other ILDs may be undiscovered, hidden beneath chaos, or removed, as the preservation potential of easily erodible uncapped subice volcanoes are low [Van Bemmelen and Rutten, 1955; Chapman et al., 2000]. If the known ILDs in Juventae are assumed to be basaltic subice volcanoes, calorimetry can be used to estimate the volumes of meltwater generated by their eruption [Allen, 1980; Björnsson, 1988; Gudmundsson and Björnsson, 1991; Gudmundsson et al., 1997; Höskuldsson and Sparks, 1997]. These estimates are based on (1) the volume and likely density of the mounds, (2) the heat content of basaltic magmas, and (3) the specific heat capacity and the latent heat of fusion for ice.

[29] The volume of meltwater ( $V_w$ ) that can be produced by a mass,  $m$ , of magma as it solidifies and cools can be calculated by equating the heat content of the magma with the heat used for ice melting. By solving for water volume we obtain:

$$V_w = \frac{m(L_m + C_m \Delta T_m)}{\rho_w (C_i (T_0 - T_i) + L_i)}. \quad (2)$$

Here,  $L_m$  is the latent heat of solidification for basaltic magma, about  $4 \times 10^5 \text{ J kg}^{-1}$  [Spera, 2000],  $C_m$  is the specific heat capacity of the basalt, about  $10^3 \text{ J kg}^{-1} \text{ K}^{-1}$  [Allen, 1980],  $\Delta T_m = 1150\text{--}1200 \text{ K}$  is a common drop from magmatic to ambient temperatures,  $\rho_w$  is density of water,  $C_i = 2 \times 10^3 \text{ J kg}^{-1}$  and  $L_i = 3.35 \times 10^5 \text{ J kg}^{-1}$  are respectively the specific heat capacity and latent heat of fusion for ice [Paterson, 1994],  $T_0$  is the temperature of the melting point for ice, and  $T_i$  is the initial ice temperature.

[30] A typical mean dry bulk density of basaltic subice volcanoes in Iceland is around  $2000 \text{ kg m}^{-3}$  [Brown et al., 1991; Gudmundsson and Milsom, 1997]. Using this

density, the mass of the three Viking-detected mounds is  $3.1 \times 10^{15} \text{ kg}$ ,  $7.6 \times 10^{14} \text{ kg}$ , and  $1.7 \times 10^{14} \text{ kg}$ . The total heat released during the formation of the mounds (the numerator in equation (1)) is estimated as  $4.9 \times 10^{21} \text{ J}$ ,  $1.2 \times 10^{21} \text{ J}$ , and  $2.7 \times 10^{20} \text{ J}$  (Table 1). Two possible cases for potential meltwater production are presented in Table 1. In the first case it is assumed that the chasma contained ice at the melting point (close to  $273 \text{ K}$ ) and in the other case the present-day temperature at the latitude of Juventae Chasma of  $150 \text{ K}$  [Haberle et al., 1999] is assumed. The water volumes presented in the table are maximum values since we assume that the total heat of the eruptions was available for melting ice. However, it is possible that some heat may have been lost to the Martian atmosphere if the eruptions broke through the ice cover. Also some heat may

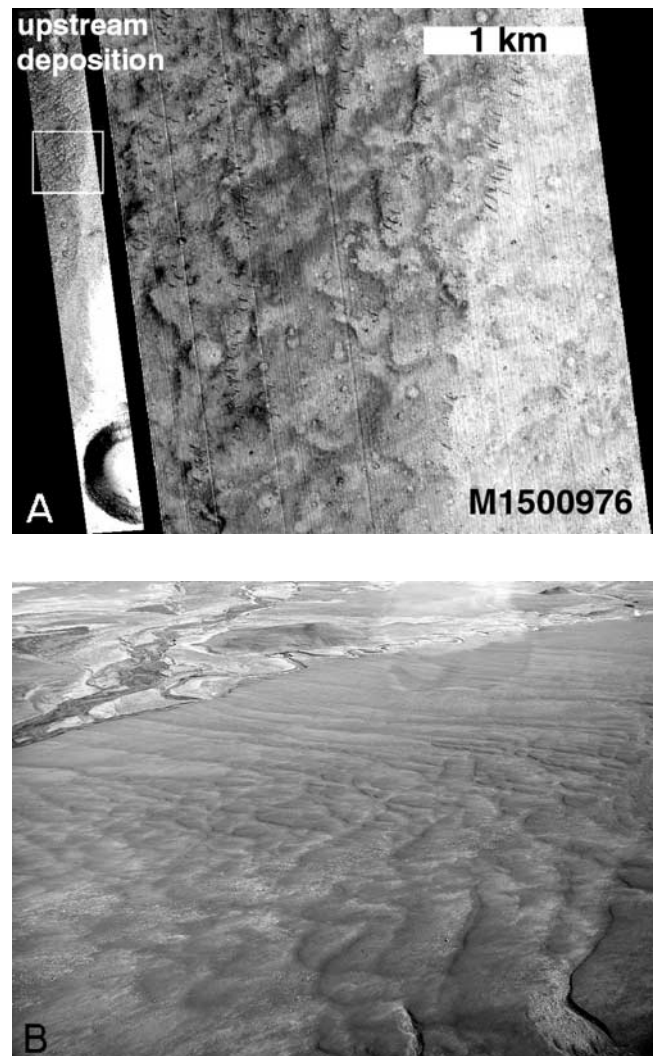


**Figure 15.** Images showing streamlined deposits with megaripples, indicating that they are depositional flood bars in (a) Maja Valles (MOC M15-00976; enlarged boxed area shows ripples indicating flow from bottom; north toward top) and in the (b) Jökulsá á Fjöllum, flood channel in northeast Iceland (flow from upper right); ripples are tens of meters wide.

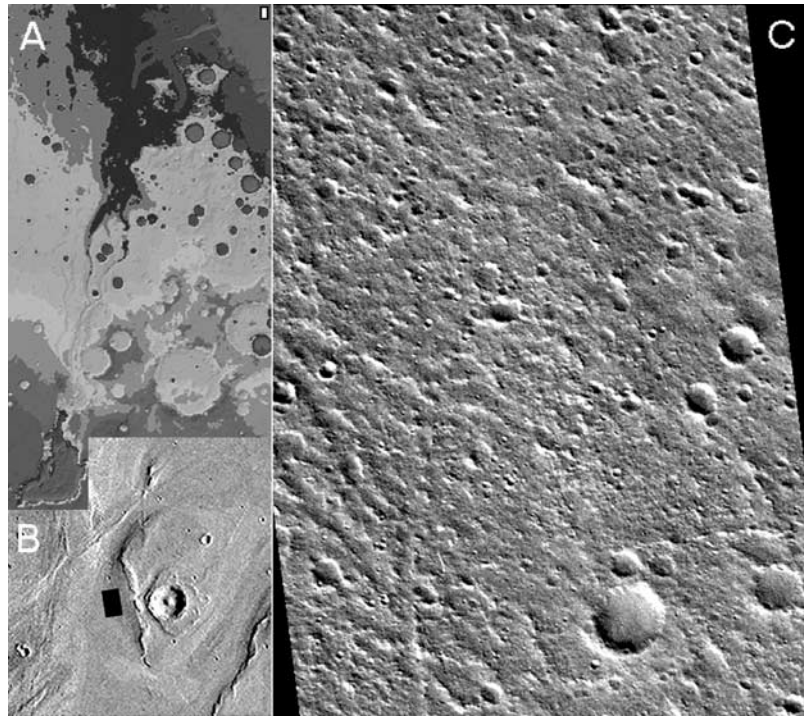


**Figure 16.** Image showing (a) box location of MOC image M10-00600 in Chryse basin at the terminus of the Maja Valles channel, on MOLA context image; (b) image location in front of streamlined island on Viking context image; and (c) part of image (1.52 km wide) showing numerous pristine impact craters; north toward top.

be lost to the surrounding ice. Nevertheless, the volumes estimates demonstrate that mound formation as monogenetic subice volcanoes could have generated  $10^3$ – $10^4$  km<sup>3</sup> of meltwater, potentially enough to cause catastrophic floods. Observations from Icelandic subglacial eruptions suggest that it is unrealistic to expect that the total volume of meltwater produced be drained in one event. Though heat may be released very rapidly during volcanic eruption [Gudmundsson *et al.*, 1997], a part of the heat is gradually released over periods that are orders of magnitude longer than the duration of the eruption [Gudmundsson and Björnsson, 1991].

[31] Flooding associated with volcanic activity in Iceland is characterized by a large initial jökulhlaup that drains a large fraction of the total produced meltwater, followed by relatively minor floods that drain the remaining volume [Gudmundsson and Björnsson, 1991; Tómasson, 1996; Gudmundsson *et al.*, 1997]. The same may be applied to Juventae Chasma. Using the empirical Clague-Mathews equation for terrestrial jökulhlaups,  $Q_{\max} = 75(V_o/10^6)^{0.67}$  [e.g., Paterson, 1994], where  $Q_{\max}$  (m<sup>3</sup>s<sup>-1</sup>) is maximum discharge and  $V_o$  (m<sup>3</sup>) is total water volume, a maximum discharge of order  $10^6$  m<sup>3</sup>/s is obtained for the largest volumes in Table 1. Thus if a mechanism existed where a large fraction of the meltwater could have been trapped until catastrophic release in a swift flood, mound formation subice volcanoes in large-volume eruptions may account for the Maja Vales flood channels.

[32] The discharge volume of  $10^6$  m<sup>3</sup>/s calculated by the above method is significantly lower than estimates using channel morphometry [Carr, 1979; De Hon and Pani, 1993;

this study]. It is an order of magnitude lower than that calculated by De Hon and Pani [1993] and 100 times lower than the maximum discharge of  $10^8$  m<sup>3</sup>s<sup>-1</sup> presented in this paper. However, if the ILDs are subice volcanoes, it may be a more realistic number, as we have no way of knowing the maximum height of the wetted channel surface relative to its current depth. Volumes determined from channel morphometry can only provide estimates of maximum discharges based on bank-full flow of the present channel and do not take into account base level erosion accrued during flow, waning flood stages, additional floods, or later wind erosion. For example, the Colorado River incised the Grand Canyon, but the maximum height of the wetted river channel surface is only a few meters, not 1.6 km to the canyon rim.

#### 4. Discussion and Conclusion

[33] MGS data has provided many new insights into the origins of the Maja Valles/Juventae Chasma system. For instance, new crater counts from MOC (N/A) images indicate variable surface ages along the length of the channel, with the channel mouth being the oldest surface. Large-scale bars with megaripples, obstacle marks and kettle holes observed on MOC images indicate the catastrophic flooding truly occurred in Maja Valles. A variably cratered streamlined island indicates at least two periods of flooding occurred at the head of the channel. Sparse impact craters near the headwater area suggest the latest flood episode may be relatively recent, perhaps Amazonian in age. Better age information was unattainable, as

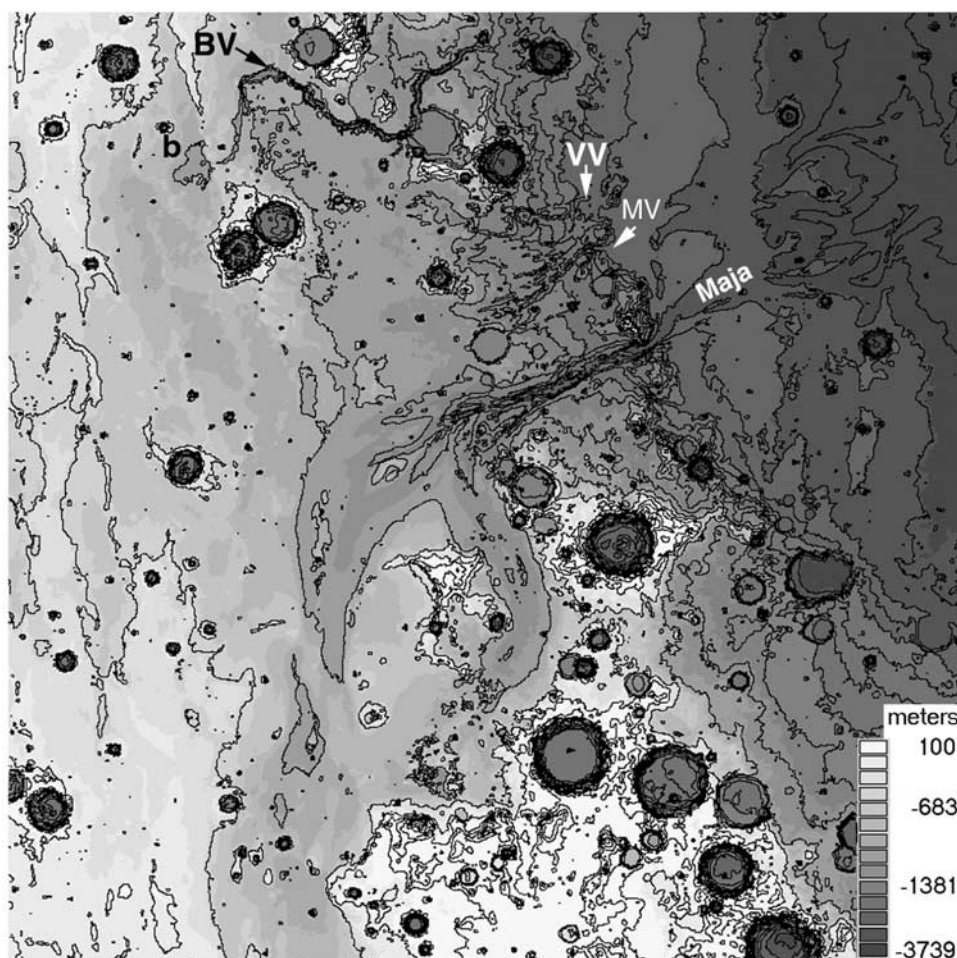


**Figure 17.** Gridded MOLA data (127 pixel/degree; 463 m/pixel) at mouth of Maja Valles; 200 m contour interval; note that there are no closed contours, indicating ponding near the terminus of the channel; north toward top; Bahram Vallis (BV), Vedra Valles (VV), Maumee Valles (MV), small basin west of Bahram Valles marked “b.”

incremental crater plots [Hartmann *et al.*, 2001] did not provide good statistics for these resurfaced areas. MOC images show evidence of late-stage ground ice in the chasma (such as thermokarst pits and brittle fracture of materials), as well as a small craterless cone that suggests recent volcanism. If the ILD mounds are subice volcanoes, then image data imply that at least two periods of flooding may be supported by at least two stages of mound formation in Juventae Chasma. MOLA topography indicates a 3-km topographic barrier to water flow between Juventae Chasma and Maja Valles. Assuming subice volcanism generated floods, it is possible to use the heights and volumes of the mound, the morphology of the chasma, and calorimetry values of known eruptions to estimate that Maja was cut by several floods having discharges of up to  $10^6$  m<sup>3</sup>/s. These floods could have been generated from melted ice, and beneath the ice they were driven by heat and the gravity potential to flow over the barrier and out of the chasma. These calculated discharges are much lower than those generated by channel morphology methods, but they may reflect more realistic estimates of flow, as channels rarely fill valleys to bank-full flood stage.

[34] Crater-count data presented in this paper suggest that floods from the youngest episode either did not reach the full extent of the channel or had very little effect on surface modification of the lower channel areas. On Lunae Planum, along the northern downstream area of Maja Valles, MOC images show no evidence of young floods and MOLA data show no topographic lows capable of ponding floodwaters.

[35] Although MOC images show clear evidence of catastrophic flooding in the mid-section of Maja Valles, we cannot rule out the possibility of debris flows and/or glacial erosion downstream. Though no evidence of flowing ice has yet been observed, the frigid temperatures of Mars, the extraordinary runouts of the circum-Chryse outflow channels, and some geomorphic features may suggest some combination of catastrophic flooding, mass flow, and glacial action [Chapman and Scott, 1989; De Hon and Pani, 1993].

[36] Catastrophic flood features in the mid-section of Maja Valles also do not rule out a pre-flood origin of the system associated with mass flows or cryoclastic flows. Some process such as volcanism or cryoclastic eruption had to create the chasma void in order to pond the ice that sourced subsequent floods. In the cryoclastic flow scenario,

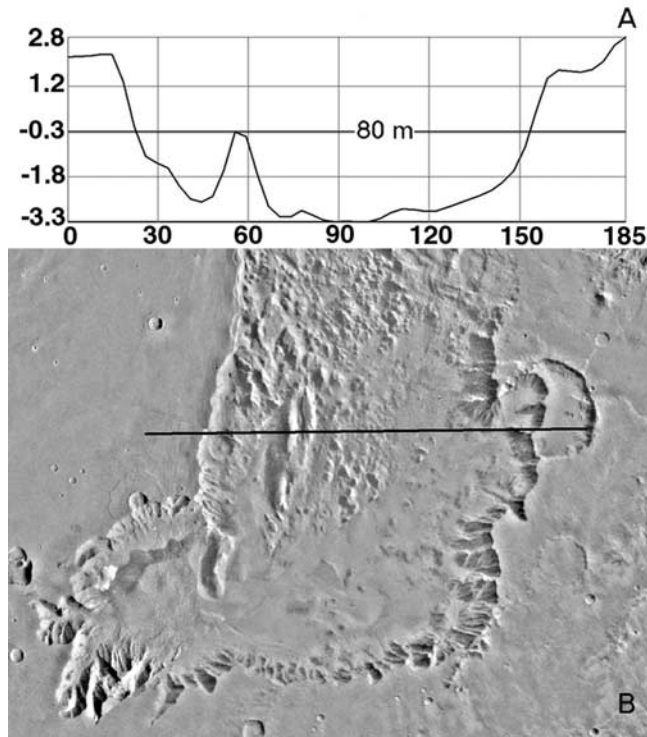


**Figure 18.** (a) MOLA relative elevation profile along EW line across largest ILD mound in Juventae Chasma; relative scale in meters; dark line indicates absolute elevation of +80 m. (b) Location of profile in Juventae Chasma; north toward top.

the initial eruption of subsurface  $\text{CO}_2$  would not preclude ice in the chasma [Chapman and Tanaka, 2002]. A  $\text{CO}_2$  aquifer, as modeled by Hoffman [2000], may overlie liquid water that could infill surface voids after  $\text{CO}_2$  eruption (N. Hoffman, personal communication, 2001) and freeze. Creation of the void by  $\text{CO}_2$  eruption, later water filling the

**Table 1.** Mass, Total Magmatic Heat Content, and Potential Meltwater Production

Interior Layered Deposit	Mass, Kg	Heat Content, J	Maximum Meltwater Production, $\text{km}^3$	
			273 K	150 K
Mound 1	$3.1 \times 10^{15}$	$4.9 \times 10^{21}$	14700	8500
Mound 2	$7.6 \times 10^{14}$	$1.2 \times 10^{21}$	3600	2100
Mound 3	$1.7 \times 10^{14}$	$2.7 \times 10^{20}$	800	460
Total	$4.0 \times 10^{15}$	$6.4 \times 10^{21}$	19100	11060

chasmata, subsequent ice melting by subice volcanism, and jökulhlaup-induced mass flows could presumably all be due to the continued rise of local magma sources to the surface [Chapman and Tanaka, 2002].

[37] Finally, new MGS data are providing information about relatively young processes in the chasma. For example, MOC images indicate a young cone of dark material that may be a volcano. These types of young vents may have produced the dark mafic deposits in the Valles Marineris chasmata. MOC N/A image crater counts indicate a very young surface age of Juventae Chasma may be due to surface modification by late-stage erosion of friable target rocks, disruption by melting of late-stage ground ice, the young mafic volcanic activity, some material subsequently removed that protected the area from impacts (dust, ice?), and recent eolian activity.

[38] Though many circum-Chryse outflow channels have multiple sources, Juventae Chasma is an isolated chasma that sourced the Maja Valles channel. These unique characteristics suggest the Juventae Chasma/Maja Valles can be considered a perhaps simpler type example of this kind of collapse-fed channel system. Additional detailed geologic mapping of the entire chasma/channel system may provide clues to help evaluate the nature, origin, and age of (1) chasmata; (2) chaotic material; (3) ILDs; and (4) outflow channels.

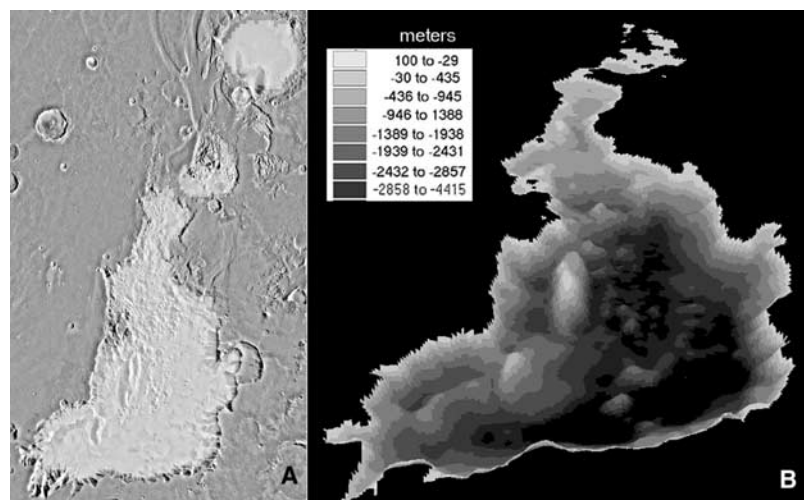


**Figure 19.** (a) Juventae Chasma and areas directly north shown infilled to absolute elevation of +80 m (white semitransparent fill). (b) MOLA topography of features within Juventae Chasma below the absolute elevation of + 80 m. North toward top.

[39] **Acknowledgments.** We are grateful to Jim Skinner, Dave MacKinnon, Goro Komatsu, and Gian Ori for their comments and contributions toward this manuscript. We would also like to thank Jim Skinner for his help in converting MOC images into ISIS format. Thanks also to Eric Noreen for providing MOLA GIS-base estimates of ILD mound volumes. All Mars Orbiter Camera images are courtesy of Malin Space Science Systems.

## References

- Allen, C. C., Icelandic subglacial volcanism—Thermal and physical studies, *J. Geol.*, **88**, 108–117, 1980.
- Allen, J. R. L., *Sedimentary Structures, Their Character and Physical Basis*, vol. 2, Elsevier Sci., New York, 1984.
- Anderson, R. C., J. M. Dohm, M. P. Golombek, A. F. C. Haldemann, B. J. Franklin, K. L. Tanaka, J. Lias, and B. Peer, Primary centers and secondary concentrations of tectonic activity through time in the western hemisphere of Mars, *J. Geophys. Res.*, **106**, 20,563–20,585, 2001.
- Baker, V. R., Erosional processes in channelized water flows on Mars, *J. Geophys. Res.*, **84**, 7895–7993, 1979.
- Baker, V. R., and D. J. Kochel, Martian channel morphology: Maja and Kasei Valles, *J. Geophys. Res.*, **84**, 7961–7984, 1979.
- Baker, V. R., and D. J. Milton, Erosion by catastrophic floods on Mars and Earth, *Icarus*, **23**, 27–41, 1974.
- Björnsson, H., Hydrology of ice caps in volcanic regions, *Soc. Sci. Isl.*, **45**, 137 pp., 1988.
- Brown, G. C., S. P. Everett, H. Rymer, D. W. McGarvie, and I. Foster, New light on caldera evolution—Askja, Iceland, *Geology*, **19**, 352–355, 1991.
- Carr, M. H., Tectonism and volcanism of the Tharsis region of Mars, *J. Geophys. Res.*, **79**, 3943–3949, 1974.
- Carr, M. H., Formation of Martian flood features by release of water from confined aquifers, *J. Geophys. Res.*, **84**, 2995–3007, 1979.
- Carr, M. H., *The Surface of Mars*, 232 pp., Yale Univ. Press, New Haven, Conn., 1981.
- Chapman, M. G., Evidence, age, and thickness of a frozen paleolake in Utopia Planitia, Mars, *Icarus*, **109**, 393–406, 1994.
- Chapman, M. G., A Martian equivalent of a fragile Earth environment, paper presented at GSA/GSL Global Meeting, Edinburgh, Geol. Soc. of Am., Geol. Soc. of London, 24–28 June 2001.
- Chapman, M. G., Layered, massive, and thin sediments on Mars: Possible late Noachian to late Amazonian tephra?, *Geol. Soc. London, Spec. Publ.*, **202**, 273–293, 2002.
- Chapman, M. G., and A. J. Russell, Juventae Chasma/Maja Valles, Mars: Implications of MOC cratering densities and geomorphology, *Geol. Soc. Am.*, **33**(6), A432, 2001.
- Chapman, M. G., and D. H. Scott, Geology and hydrology of the north Kasei Valles area, Mars, *Proc. Lunar Planet. Sci. Conf.*, **19**, 367–375, 1989.
- Chapman, M. G., and J. L. Smellie, Putative large and small volcanic edifices in Valles Marineris, Mars and evidence of ground water/ice, *Eos Trans. AGU*, Fall Meet. Suppl., Abstract P21C-11, F698, 2001.
- Chapman, M. G., and K. L. Tanaka, Interior trough deposits on Mars: Sub-ice volcanoes?, *J. Geophys. Res.*, **106**(E5), 10,087–10,000, 2001.
- Chapman, M. G., and K. L. Tanaka, Related magma-ice interactions: Possible origins of chasmata, chaos, outflow channels, and surface materials in Xanthe, Margaritifer, and Meridiani Terrae, Mars, *Icarus*, **155**, 324–339, 2002.
- Chapman, M. G., C. C. Allen, M. T. Gudmundsson, V. C. Gulick, S. P. Jakobsson, B. K. Lucchitta, I. P. Skilling, and R. B. Waitt, Volcanism and ice interactions on Earth and Mars, in *Deep Oceans to Deep Space: Environmental Effects on Volcanic Eruptions*, edited by T. K. P. Gregg and J. R. Zimbelman, pp. 39–74, Plenum, New York, 2000.
- Chow, V. T., *Open Channel Hydraulics*, 680 pp., McGraw-Hill, New York, 1959.
- Croft, S. K., Geologic map of the Hebes Chasma quadrangle, VM 500K 00077 (abstract), *NASA TM 4210*, pp. 539–541, NASA, Greenbelt, Md., 1990.
- Cutts, J. A., and K. R. Blasius, Origin of Martian outflow channels—The eolian hypothesis, *J. Geophys. Res.*, **86**, 5061–5074, 1981.
- De Hon, R. A., Geologic map of the Pompeii quadrangle (MTM 20057), Maja Valles region of Mars, *USGS Misc. Invest. Ser. Map I-2203*, scale 1:500000, U.S. Geol. Surv., Reston, Va., 1992.
- De Hon, R. A., and E. A. Pani, Flood surge through the Lunae Planum outflow complex, Mars, *Proc. Lunar Planet. Sci. Conf.*, **22**, 63–71, 1993.
- Fay, H., The formation of ice-block obstacle marks during the November 1996 glacier outburst flood (jökulhlaup), Skeidarársandur, southern Iceland, in *Flood and Megaflood Deposits: Recent and Ancient, Spec. Publ. Int. Assoc. Sedimentol.*, vol. 32, edited by I. P. Martini, V. R. Baker, and G. Garzon, pp. 85–97, Int. Assoc. Sedimentol., Gent, Belgium, 2002a.
- Fay, H., Formation of kettle holes following a glacial outburst flood (jökulhlaup), Skeidarársandur, southern Iceland, in *The Extremes of the Extremes: Extraordinary Floods, Int. Assoc. Hydrol. Sci. Publ.*, vol. 271, edited by A. Snorasson, H. P. Finnsdóttir, and M. Moss, pp. 205–210, Int. Assoc. Hydrol. Sci., Gent, Belgium, 2002b.
- French, H. M., *The Periglacial Environment*, 341 pp., Addison Wesley Longman, New York, 1996.
- Geissler, P. E., R. B. Singer, and B. K. Lucchitta, Dark materials in Valles Marineris: Indications of the style of volcanism and magmatism on Mars, *J. Geophys. Res.*, **95**, 14,399–14,413, 1990.
- Gooding, J. L., Undercooled water in basaltic regoliths and implications for fluidized debris flows on Mars, *Icarus*, **72**, 519–527, 1987.
- Greeley, R., E. Theilig, J. E. Guest, M. H. Carr, H. Masursky, and J. A. Cutts, The geology of Chryse Planitia, *J. Geophys. Res.*, **82**, 4093–4110, 1977.
- Gudmundsson, M. T., and H. Björnsson, Eruptions in Grimsvötn 1983, Vatnajökull, Iceland, 1934–1991, *Jökull*, **41**, 21–45, 1991.
- Gudmundsson, M. T., and J. Milsom, Gravity and magnetic studies of the subglacial Grimsvötn volcano, Iceland: Implications for crustal and thermal structure, *J. Geophys. Res.*, **102**, 7691–7704, 1997.
- Gudmundsson, M. T., F. Sigmundsson, and H. Björnsson, Ice-volcano interaction of the 1996 Gjalp subglacial eruption, Vatnajökull, Iceland, *Nature*, **389**, 954–957, 1997.
- Haberle, R. M., M. M. Joshi, J. R. Murphy, J. R. Barnes, J. T. Schofield, G. Wilson, M. Lopez-Valverde, J. L. Hollingsworth, A. F. C. Bridger, and J. Schaeffer, General circulation model simulations of the Mars Pathfinder atmospheric structure investigation/meteorology data, *J. Geophys. Res.*, **104**, 8957–8977, 1999.
- Hartmann, W. K., Martian surface and crust: Review and synthesis, *Icarus*, **19**, 550–575, 1973.
- Hartmann, W. K., Interplanetary correlation of geologic time using cratering data (abstract), presented at 33rd Lunar and Planetary Science Conference, Lunar and Planet. Inst., Houston, Tex., 2002.
- Hartmann, W. K., J. Anquita, M. A. de la Casa, D. C. Berman, and E. V. Ryan, Martian cratering 7: The role of impact gardening, *Icarus*, **149**, 37–53, 2001.
- Hoffman, N., White Mars: A new model for Mars' surface and atmosphere based on CO<sub>2</sub>, *Icarus*, **146**, 326–342, 2000.
- Höskuldsson, A., and R. S. J. Sparks, Thermodynamics and fluid dynamics of effusive subglacial eruptions, *Bull. Volcanol.*, **59**, 219–230, 1997.
- Jones, J. G., Intraglacial volcanoes of the Laugarvatn region, south-west Iceland, *Geol. Soc. London Q. J.*, **124**, 197–211, 1969.
- Jones, J. G., Intraglacial volcanoes of the Laugarvatn region, south-west Iceland, II, *J. Geol.*, **78**, 127–140, 1970.
- Jöns, H. P., Das relief des Mars: Versuch einer zusammenfassenden übersicht, *Geol. Rundsch.*, **79**, 131–164, 1990.
- Komatsu, G., P. E. Geissler, R. G. Strom, and R. B. Singer, Stratigraphy and erosional landforms of layered deposits in Valles Marineris, Mars, *J. Geophys. Res.*, **98**, 11,105–11,121, 1993.
- Lucchitta, B. K., Ice sculpture in the Martian outflow channels, *J. Geophys. Res.*, **87**, 9951–9973, 1982.
- Lucchitta, B. K., Young volcanic deposits in the Valles Marineris, Mars, *Icarus*, **86**, 476–509, 1990.
- Lucchitta, B. K., Late mafic volcanism in Valles Marineris, Mars, *Eos Trans. AGU*, **82**(20), Fall Meet. Suppl., Abstract P32C-0563, 2001.
- Lucchitta, B. K., G. D. Clow, P. E. Geissler, A. S. McEwen, R. A. Schultz, R. B. Singer, and S. W. Squyres, The canyon system on Mars, in *Mars*, edited by H. H. Kieffer et al., pp. 453–492, Univ. of Ariz. Press, Tucson, 1992.
- Lucchitta, B. K., N. K. Isbell, and A. Howington-Kraus, Topography of Valles Marineris: Implications for erosional and structural history, *J. Geophys. Res.*, **99**, 3783–3798, 1994.
- MacKinnon, D. J., and K. L. Tanaka, The impacted Martian crust: Structure, hydrology, and some geologic implications, *J. Geophys. Res.*, **94**, 17,359–17,370, 1989.
- Masursky, H., J. M. Boyce, A. L. Dial Jr., G. G. Schaber, and M. E. Stobell, Classification and time of formation of Martian channels based on Viking data, *J. Geophys. Res.*, **82**, 4016–4038, 1977.
- McCaughey, J. F., M. H. Carr, J. A. Cutts, W. K. Hartman, H. Masursky, D. J. Milton, R. P. Sharp, and D. E. Wilhelms, Preliminary Mariner 9 report of the geology of Mars, *Icarus*, **17**, 289–327, 1972.
- Milton, D. J., Water and processes of degradation in the Martian landscape, *J. Geophys. Res.*, **78**, 4037–4047, 1973.
- Nedell, S. S., S. W. Squyres, and D. W. Andersen, Origin and evolution of the layered deposits in the Valles Marineris, Mars, *Icarus*, **70**, 409–441, 1987.
- Nummedal, D., and D. B. Prior, Generation of Martian chaos and channels by debris flows, *Icarus*, **45**, 77–86, 1981.
- Paterson, W. S. B., *The Physics of Glaciers*, 3rd ed., 4800 pp., Pergamon, New York, 1994.

- Rice, J. W., Jr., and R. A. De Hon, Geologic map of the Darvel quadrangle (MTM 20052), Maja Valles region of Mars, *USGS Misc. Invest. Ser. Map I-2432*, scale 1:500000, U.S. Geol. Surv., Reston, Va., 1996.
- Rice, J. W., Jr., and K. S. Edgett, Catastrophic flood sediments in Chryse Basin, Mars, and Quincy Basin, Washington: Application of sandar facies model, *J. Geophys. Res.*, *102*, 4185–4200, 1997.
- Rotto, S., and K. L. Tanaka, Geologic/Geomorphic map of the Chryse Planitia region of Mars, *USGS Misc. Invest. Ser. Map I-2441*, scale 1:5000000, U.S. Geol. Surv., Reston, Va., 1995.
- Russell, A. J., Obstacle marks produced by flows around stranded ice blocks during a jökulhlaup in West Greenland, *Sedimentology*, *40*(6), 1091–1113, 1993.
- Russell, A. J., and Ó. Knudsen, The influence of flow stage on the morphology and sedimentology of November 1996 jökulhlaup deposits, Skeiðarársandur, Iceland, in *Flood and Megaflood Deposits: Recent and Ancient, Spec. Publ. Int. Assoc. Sedimentol.*, vol. 32, edited by I. P. Martini, V. R. Baker, and G. Garzon, pp. 67–83, Int. Assoc. Sedimentol., Gent, Belgium, 2002.
- Schofield, J. T., J. R. Barnes, D. Crisp, R. M. Haberle, S. Larsen, J. A. Magalhães, J. R. Murphy, A. Seiff, and G. Wilson, The Mars Pathfinder Atmospheric Structure Investigation/Meteorology (ASI/MET) experiment, *Science*, *278*, 1752–1758, 1997.
- Scott, D. H., and K. L. Tanaka, Geologic map of the western equatorial region of Mars, *USGS Misc. Invest. Ser. Map I-1802-A*, 1:15000000 scale, U.S. Geol. Surv., Reston, Va., 1986.
- Sharp, R. P., Mars—Troughed terrain, *J. Geophys. Res.*, *78*(20), 4063–4072, 1973.
- Sharp, R. P., and M. C. Malin, Channels on Mars, *Geol. Soc. Am. Bull.*, *86*, 593–609, 1975.
- Spera, F. J., Physical properties of magmas, in *Encyclopedia of Volcanoes*, edited by H. Sigurdsson, pp. 171–190, Academic, San Diego, Calif., 2000.
- Sugden, D. E., and B. S. John, *Glaciers and Landscape*, 376 pp., Arnold, London, 1976.
- Tanaka, K. L., Sedimentary history and mass flow structures of Chryse and Acidalia Planitiae, Mars, *J. Geophys. Res.*, *102*, 4131–4149, 1997.
- Tanaka, K. L., M. P. Golombek, and W. B. Banerdt, Reconciliation of stress and structural histories of the Tharsis region of Mars, *J. Geophys. Res.*, *96*, 15,617–15,633, 1991.
- Tanaka, K. L., J. S. Kargel, D. J. MacKinnon, T. M. Hare, and N. Hoffman, Catastrophic erosion of Hellas basin rim on Mars induced by magmatic intrusion into volatile-rich rocks, *Geophys. Res. Lett.*, *29*(8), 1195, doi:10.1029/2001GL013885, 2002.
- Theilig, E., and R. Greeley, Plains and channels in the Lunae Planum—Chryse Planitia region of Mars, *J. Geophys. Res.*, *84*, 7994–8010, 1979.
- Tómasson, H., The jökulhlaup of Katla in 1918, *Ann. Glaciol.*, *22*, 249–254, 1996.
- U.S. Geological Survey, Topographic maps of the western, eastern equatorial and polar regions of Mars, *USGS Misc. Invest. Ser. Map I-2030*, 1:15000000 scale, Reston, Va., 1989.
- Van Bemmelen, R. W., and M. G. Rutten, *Table Mountains of Northern Iceland*, E. J. Brill, Leiden, Netherlands, 217 pp., 1955.
- Wise, D. U., M. P. Golombek, and G. E. McGill, Tharsis province of Mars: Geologic sequence, geometry, and a deformation mechanism, *Icarus*, *38*, 456–472, 1979.
- Witbeck, N. E., K. L. Tanaka, and D. H. Scott, The geologic map of the Valles Marineris region, Mars, *USGS Misc. Invest. Ser. Map I-2010*, scale 1:2000000, U.S. Geol. Surv., Reston, Va., 1991.

---

M. G. Chapman and T. M. Hare, U.S. Geological Survey, 2255 N. Gemini Drive, Flagstaff, AZ 86001, USA. (mchapman@usgs.gov; thare@usgs.gov)

M. T. Gudmundsson, Raunvisindastofnun Háskólans, Science Institute, University of Iceland, Hofsvallagata 53, IS-107, Reykjavik, Iceland. (mtg@raunvis.hi.is)

A. J. Russell, Earth Surface Processes Research Group, School of Earth Sciences and Geography, Keele University, Keele, Staffordshire ST5 5BG, UK. (a.j.russell@esci.keele.ac.uk)